KAERI/TR-779/96

Mechanical Impacts of Poloidal Eddy Currents on the Continuous Vacuum Vessel of a Tokamak

1996. 11

Korea Atomic Energy Research Institute

제출문

한국원자력연구소 소장 귀하

본 보고서를

Mechanical Impacts of Poloidal Eddy Currents
on the Continuous Vacuum Vessel of a Tokamak

에 관한 기술보고서로 제출합니다.

1996 년 11 월

연구자 : 인 상 렬 (핵융합로 연구실, 책임연구원)

윤 병 주 (핵융합로 연구실, 선임연구원)

감수자 : 황 철 규 (핵융합로 연구실, 책임연구원)

ABSTRACT

Poloidal eddy currents are induced on the continuous torus vacuum vessel by changes of the toroidal field during the machine start-up(toroidal field coil charge), shut-down(toroidal field coil discharge) and plasma disruption(plasma diamgnetism change). Analytic forms for the eddy currents flowing on the vessel, consequent pressures and forces acting on it are presented in this report. The results are applied to typical operation modes of the KT-2 tokamak.

Stress analysis for two typical operation modes of toroidal field damping during a machine shut-down and plasma energy quench during a plasma disruption were carried out using 3D FEM code(ANSYS 5.2).

Contents

List of Tables

List of Figures

Mechanical impacts of poloidal eddy currents on the continuous vacuum vessel of a tokamak

Abstract

Poloidal eddy currents are induced on the continuous torus vacuum vessel by changes of the toroidal field during the machine start-up(toroidal field coil charge), shut-down(toroidal field coil discharge) and plasma disruption(plasma diamgnetism change). Analytic forms for the eddy currents flowing on the vessel, consequent pressures and forces acting on it are presented in this report. The results are applied to typical operation modes of the KT-2 tokamak.

Stress analysis for two typical operation modes of toroidal field damping during a machine shut-down and plasma energy quench during a plasma disruption were carried out using 3D FEM code(ANSYS 5.2).

I. Introduction

One of the critical considerations in tokamak design for mechanical engineers, electrical engineers and plasma physicists is the effect of eddy currents induced on the vacuum vessel. Vessel eddy currents are induced due to transient magnetic fields in practically every tokamak operation stage. The eddy currents may give rise to damaging forces in the vessel structure[1,2,3].

During plasma initiation, vertical displacement and plasma current quench, variations of poloidal magnetic fields produce toroidal vessel currents, while poloidal vessel currents are generated due to changes of the toroidal magnetic field in the stages of TF(toroidal field) rising and TF damping. The change of poloidal beta and consequent variation of plasma diamagnetism in a plasma disruption also produces poloidal eddy currents on the vessel. The vessel currents interact with magnetic fields orthogonal to them, and the resultant electromagnetic load is perpendicular to the vessel surface. In addition to the mechnical impacts the eddy currents also inhibit plasma formation, equilibrium field ramp-up and plasma active control. They, however, help fast passive control of the plasma and shield magnets placed outside the vessel from electromagnetic transient. The practical level of the effect of the vessel eddy current depends on the relative magnitude of the magnetic field diffusion(or current decay) time constant compared with the change rate of the applied field. The longer

the diffusion time is, the stronger the effect is.

This report describes the procedure of estimating the effect of vessel poloidal eddy currents produced by the changes of the toroidal field due to any causes. In Sec. II general expressions for the eddy currents induced on the all-welded torus vacuum vessel and pressures acting on the vessel when the toroidal field coil is charged or discharged. The mode of the diamagnetic change in a plasma disruption is considered in Sec. III. Application of the results on the KT-2 tokamak is found in each section. Finally, the results of the stress analysis in TF damping and plasma energy quench as typical operation modes producing poloidal eddy currents are discussed in Sec. IV.

II. Charging and discharging the toroidal field coil[4]

Figure 1 shows a toroidal field coil modeled as a current sheet and a conducting torus shell located inside the coil. The coil and the vessel have arbitrary cross-sections.

Before start-up($t<0$) the field is zero on both sides of the vessel, while the coil field B exists in the steady state with the toroidal field coil charged fully. The field inside the vessel starts to increase or decrease as the coil is charged or discharged. There may be delays in feeling the field change inside the vessel due to the finite field diffusion time depending on the vessel material and geometry. The toroidal field is usually varied so slowly that it may be assumed to be a quas-steady one. That is, the field inside the vessel is just the same field applied by the toroidal field coil, without any delay and any distortion, except minor contribution from vessel currents.

The locally induced magnetic pressure is given by Equation (1).

$$P = J_v \left(B_t + \frac{B_i}{2} \right) t_v \qquad (1)$$

where, P: magnetic pressure acting on the vessel at a observing point(=P(r))[Pa]

J_v: current density flowing on the vessel(=J_v(r))[A/m^2]

B_t: magnetic field applied by toroidal field coil(=B_t(r))[T]

B_i: magnetic field induced by the vessel eddy currents(=B_i(r))[T], 1/2 is introduced because the poloidal current does not produce toroidal field outside the current shell, then in the vessel wall B_i is assumed to be changed linearly from zero at the outer surface to the full value at the inner surface

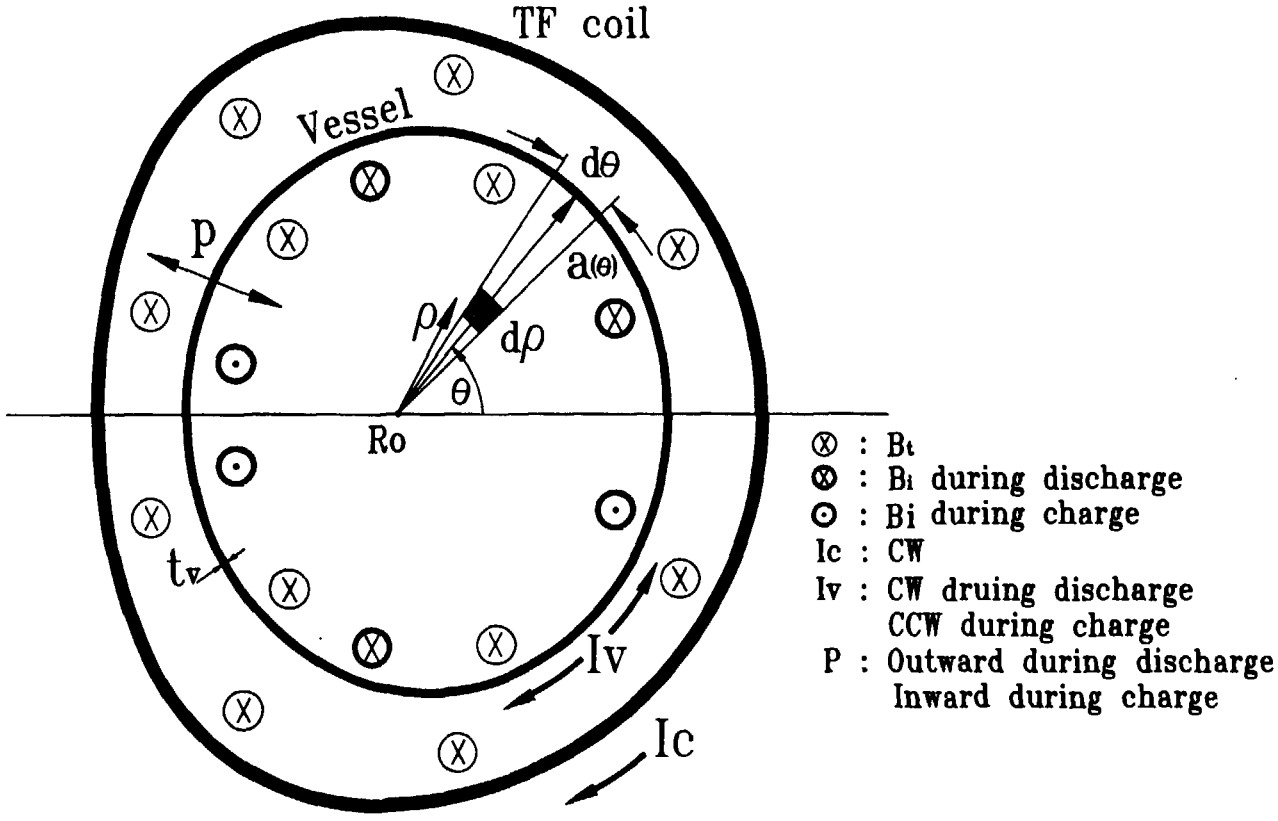

Fig.1. Current and pressure induced on a vessel placed within a toroidal field coil.

t_v: thickness of the vessel wall[m]

r: major radius to the point in question[m].

The pressure is composed of two terms($P=P_o+P_i$), one from the applied field($P_o=J_vB_tt_v$) and the other from the induced field($P_i=J_vB_it_v/2$). The direction of the pressure depends on the directions of the vessel current and the magnetic field. The direction of B_t is not changed in spite of variation in the magnitude, and that of induced current depends on the sign of change rate of B_t. The first term has minus sign(inward) when the field decreases, and plus(outward) when the field increases. The second term has always plus because the induced field has the same sign as the vessel current. The magnitude of the second term is expected to be much lower than the first term because it is second-order.

The power supply of the toroidal field coil may be considered as a constant voltage source. Because the coil is a inductive load the coil current and the field varies in accordance with a exponential function. To shorten the time taken to reach the flat top power supply voltage is increased a little higher(a few tens percent) than a steady one at the flat top. The ratio of the two volages is called overvoltage or forcing factor and is denoted usually by α. If the toroidal field coil is charged from zero according to Equation (2), we can obtain expressions of J_v, B_i and consequently P in Equation (1) step by step.

$$B_t = \alpha B_{t0} \frac{R_p}{r} (1-e^{-t/\tau}) \tag{2}$$

where, α: overvoltage factor(=supplied voltage/flat-top voltage)

B_{t0}: flat-top mafnetic field at the plasma center[T]

R_p: major radius to the plasma center[T]

τ: time constant of the coil(=L_c/R_c, L_c is the coil inductance and R_c is the coil resistance)[sec]

t: time[sec]

The induced vessel poloidal current is governed by the circuit equation as follows,

$$L_v \frac{dI_v}{dt} + R_vI_v = - \frac{d\Phi}{dt} \tag{3}$$

where, L_v: poloidal inductance of the vessel[H]

R_v: poloidal resistance[Ω]

I_v: vessel poloidal current(=$2\pi r t_v J_v(r)$)[A]

Φ: magnetic flux linking the cross-section of the vessel[Wb].

Φ is obtained by integrating applied magnetic field over the cross-sectional area of the vessel and is given by Equation (4)(refer to Fig. 1 for notations of the variables used in the equation).

$$\Phi = \int B_t \, dA = \alpha B_{t0} R_p (1-e^{-t/\tau}) \int \frac{dA}{r}$$

$$= \alpha B_{t0} R_p (1-e^{-t/\tau}) \int_0^{2\pi} \int_0^a \frac{\rho \, d\rho \, d\theta}{R_0 + \rho \cos\theta} = CF(1-e^{-t/\tau}) \qquad (4)$$

where, a: minor radius to the vessel wall(=$a(\theta)$)[m]

ρ: minor radius to the infinitesimal element of surface integration[m]

R_0: major radius to the vessel center[m]

C: constant(=$\alpha B_{t0} R_p$)

F: double integral term.

L_v and R_v are calculated by the vessel geometry and are expressed by Equations (5) and (6) respectively.

$$L_v = \frac{d\Phi_v}{dI_v} = \frac{\mu_0}{2\pi} F \qquad (5)$$

where, Φ_v: flux linking the vessel cross-section, generated by the vessel current[Wb]

μ_0: permeability in vacuum.

$$R_v = \int \frac{\eta \, d\ell}{2\pi r t_v} = \frac{\eta}{2\pi t_v} \int_0^{2\pi} \frac{\sqrt{(a^2 d\theta^2 + da^2)}}{R_0 + a\cos\theta} \approx \frac{\eta}{2\pi t_v} \int_0^{2\pi} \frac{a \, d\theta}{R_0 + a\cos\theta} = \frac{\eta}{2\pi t_v} G \qquad (6)$$

where, η: resistivity of the vessel material[Ω.m]

G: integral term.

The induced vessel current I_v is obtained by inserting Equation (4) into Equation (3), and by solving it. I_v is given by Equation (7).

$$I_v = -\frac{\alpha B_{t0} R_p F}{\tau R_v (1 - \frac{\tau_v}{\tau})} (e^{-t/\tau} - e^{-t/\tau_v}) = -\frac{2\pi \alpha \sigma B_{t0} R_p t_v}{\tau (1 - \frac{\tau_v}{\tau})} \frac{F}{G} (e^{-t/\tau} - e^{-t/\tau_v}) \quad (7)$$

where, - sign represents the current is induced to oppose the field increase

σ : conductivity of the vessel material(=$1/\eta$)[mho/m]

τ_v: time constant of the vessel as a poloidal circuit(=$L_v/R_v = \sigma \mu_0 t_v F/G$)[sec].

Using relations $J_v = I_v/2\pi r t_v$ and $B_i = \mu_0 I_v/2\pi r$, and inserting Equations (2) and (7) into Equation (1), Equation (8) for the pressure acting on the vessel is obtained.

$$P = -\frac{\alpha^2 B_{t0}^2 R_p^2 \sigma t_v}{r^2 \tau (1 - \tau_v/\tau)} \frac{F}{G} (1 - e^{-t/\tau} - \frac{\mu_0 \sigma t_v}{2\tau (1 - \tau_v/\tau)} \frac{F}{G} (e^{-t/\tau} - e^{-t/\tau_v}))(e^{-t/\tau} - e^{-t/\tau_v}) \quad (8)$$

where, - sign indicates inward pressure on the vessel wall.

If the vessel has a circular cross-section($a(\theta) = a_v$), F and G are solved analytically; $F(\text{circular}) = 2\pi (R_0 - \sqrt{(R_0^2 - a_v^2)})$, $G(\text{circular}) = 2\pi a_v \sqrt{(R_0^2 - a_v^2)}$, and $F/G = a_v D$(D is a constant, $= 1 + A\sqrt{(A^2 - 1)} - A^2$, A is the aspect ratio of the vessel($= R_0/a_v$), $D \rightarrow 1$ when $A > 2$). From Equations (5) and (6) an intuitive expression of τ_v for circular cross-section is obtained as Equation (9).

$$\tau_v(\text{circular}) = \mu_0 \sigma t_v a_v D \quad (9)$$

The ratio τ_v/τ (equivalent to, so called, magnetic Reynolds number R_m) is negligible when the field change is so slow that the relation $\tau >> \mu_0 \sigma t_v a$ is satisfied even in non-circular cross-sections. Then Equations (7) and (8) may be changed to approximate forms (10) and (11) respectively.

$$I_v = -\frac{2\pi \alpha \sigma t_v B_{t0} R_p}{\tau (1 - \tau_v/\tau)} \frac{F}{G} e^{-t/\tau} \quad (10)$$

$$\approx -\frac{2\pi \alpha \sigma t_v B_{t0} R_p}{\tau} \frac{F}{G} e^{-t/\tau} \quad (10)'$$

$$P = -\frac{\alpha^2 B_{t0}^2 R_p^2 \sigma t_v}{r^2 \tau (1 - \tau_v/\tau)} \frac{F}{G} (1 - (1 + \frac{\mu_0 \sigma t_v}{2\tau (1 - \tau_v/\tau)} \frac{F}{G}) e^{-t/\tau}) e^{-t/\tau} \quad (11)$$

$$\approx -\frac{\alpha^2 B_{t0}^2 R_p^2 \sigma t_v}{r^2 \tau}\frac{F}{G}(1-(1+\frac{\mu_0 \sigma t_v}{2\tau}\frac{F}{G})e^{-t/\tau})e^{-t/\tau} \qquad (11)'$$

The pressure calculated by Equation (11)' is minus for the period of $0 \leqq t < \tau \ln(1+R_m/2) \approx \tau_v/2$ (maximum error is $-\alpha^2 R_p^2 R_m^2 B_{t0}^2/2\mu_0 r^2$ at t=+0), where R_m is defined as $R_m = \tau_v/\tau = \sigma \mu_0 t_v F/\tau G$, and final error at t>>0 is about R_mx100 % arising from deletion of the term $(1-\tau/\tau_v)$. The pressure has a maximum of $\alpha^2 R_p^2 (R_m/(2+R_m)) B_{t0}^2/2\mu_0 r^2$ at $t=\tau \ln(2+R_m) \approx \tau \ln 2$ (note, here, $e^{-t/\tau} \sim 0.5$). $R_m << 1$ (or $\tau >> \tau_v$) is usaually satisfied and the error is negligible around the maximum. In Equation (11) the ratio P_i/P_o (as defined in the explanation on Equation (1)) is obtained to be $R_m/2$, which indicates the term P_i can be neglected safely. Then Equation (11) is changed to the more simplified form Equation (12).

$$P = -\frac{\alpha^2 B_{t0}^2 R_p^2 \sigma t_v}{r^2 \tau (1-\tau_v/\tau)}\frac{F}{G}(1-e^{-t/\tau})e^{-t/\tau} \qquad (12)$$

$$\approx -\frac{\alpha^2 B_{t0}^2 R_p^2 \sigma t_v}{r^2 \tau}\frac{F}{G}(1-e^{-t/\tau})e^{-t/\tau} \qquad (12)'$$

The maximum of Equation (12)', P_m, is easily solved and is given by Equation (13) which is used generally for fast estimation of the pressure..

$$P_m = -\frac{\alpha^2 B_{t0}^2 R_p^2 \tau_v}{4\mu_0 r^2 \tau} \qquad (13)$$

Discharging toroidal field coil is equivalent to simple dump of the coil current to a resister, and toroidal field decays exponentially as $B_t = (B_{t0} R_p/r) e^{-t/\tau}$. The vessel current has the same form as that of charging stage except that the magnitude is less by $1/\alpha$ and the sign is plus. The pressure is given by Equation (14), slightly different from Equation (8).

$$P = \frac{B_{t0}^2 R_p^2 \sigma t_v}{r^2 \tau (1-\tau_v/\tau)}\frac{F}{G}(e^{-t/\tau}+\frac{\mu_0 \sigma t_v}{2\tau(1-\tau_v/\tau)}\frac{F}{G})(e^{-t/\tau}-e^{-t/\tau_v}))(e^{-t/\tau}-e^{-t/\tau_v}) \qquad (14)$$

And if again $\tau >> \tau_v$, we get following equation.

$$P = \frac{B_{t0}^2 R_p^2 \sigma t_v}{r^2 \tau}\frac{F}{G}(1+\frac{\mu_0 \sigma t_v}{2\tau}\frac{F}{G})e^{-2t/\tau} \qquad (15)$$

The maximum pressure is $R_p^2 R_m(2+R_m)B_{t0}^2/2\mu_0 r^2$ at t=0. It is about $4/\alpha^2$ times larger than that of charging phase.

F in Equation (5) and G in Equation (6) have a variable $a(\theta)$ calculated along the boundary of the vessel cross-section. If the boundary is described with single- or multi-function well defined, F and G may be solved analytically, otherwise they are obtained numerically. Let's consider a practical example with the design parameters of the vessel of the KT-2 device. Figure 2 shows details of the vessel boundary which consists of three arcs and one straight[5]. For solving F it is convenient to convert the double integral to a single one as depicted in Fig. 3. Then, F is solved as Equation (16).

$$F = \int \frac{dA}{r} = 2\int_0^{\varepsilon} \frac{a_1^2 \sin^2\theta \, d\theta}{R_1 + a_1\cos\theta} + 2\int_{\varepsilon}^{\pi} \frac{a_2 \sin\theta\,(a_2\sin\theta + z_2)d\theta}{R_2 + a_2\cos\theta} =$$

$$2\left(R_1\theta - a_1\sin\theta - 2\sqrt{(R_1^2-a_1^2)}\tan^{-1}\frac{\tan(\theta/2)\sqrt{(R_1^2-a_1^2)}}{R_1 + a_1}\right)\Big|_0^{\varepsilon} +$$

$$2\left(R_2\theta - a_2\sin\theta - 2\sqrt{(R_2^2-a_2^2)}\tan^{-1}\frac{\tan(\theta/2)\sqrt{(R_2^2-a_2^2)}}{R_2 + a_2} - z_2\ln(R_2+a_2\cos\theta)\right)\Big|_{\varepsilon}^{\pi} \quad (16)$$

G is given by Equation (17).

$$G = \int \frac{d\ell}{r} = 2\int_0^{\varepsilon} \frac{a_1 d\theta}{R_1 + a_1\cos\theta} + 2\int_{\varepsilon}^{\pi} \frac{a_2 d\theta}{R_2 + a_2\cos\theta} + 2z_2/(R_2-a_2) =$$

$$\frac{2a_1}{\sqrt{(R_1^2-a_1^2)}}\tan^{-1}\frac{\tan(\theta/2)\sqrt{(R_1^2-a_1^2)}}{R_1 + a_1}\Big|_0^{\varepsilon} +$$

$$\frac{2a_2}{\sqrt{(R_2^2-a_2^2)}}\tan^{-1}\frac{\tan(\theta/2)\sqrt{(R_2^2-a_2^2)}}{R_2 + a_2}\Big|_{\varepsilon}^{\pi} + 2z_2/(R_2-a_2) \quad (17)$$

Table 1 summaries some parameters of the vessel geometry, material and the toroidal field(refer to the notations in the Fig. 3 for geometry parameters)[2,3]. In this special case F=0.667 and G=1.7657. The inductance and resistance of the vessel in the poloidal direction are 1.334×10^{-7} H and 1.639×10^{-5} Ω. The time constant of the vessel as a electrical circuit, τ_v, is 8.14 msec, which is much shorter than that of the toroidal coil, τ, and R_m is about

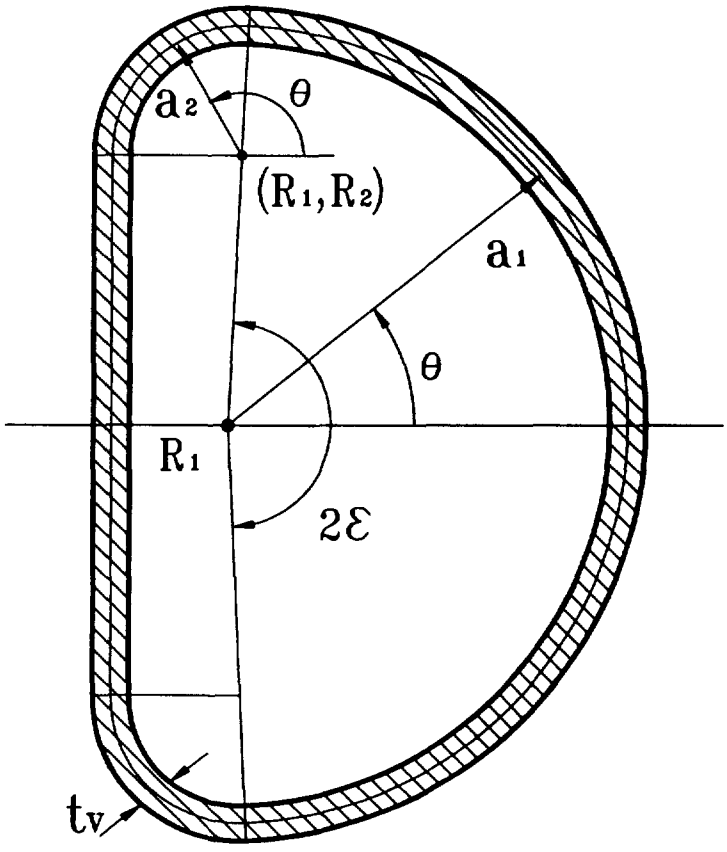

Fig.2. Schematic of the KT-2 vacuum vessel.

Table 1. Parameters for calculating induced vessel currents and pressures.

α	1.5
B_{t0}	3 Tesla
R_p	1.4 m
τ	2.86 sec
t_v	0.012 m
R_1	1.2495 m
a_1	0.6645 m
R_2	1.27 m
a_2	0.214 m
z_2	0.45 m
ε	87.4 ° (1.5254 radian)
η (ss 304L)	7×10^{-7} Ω.m
R_v	1.639×10^{-5} Ω
L_v	1.334×10^{-7} H
τ_v	8.14 msec

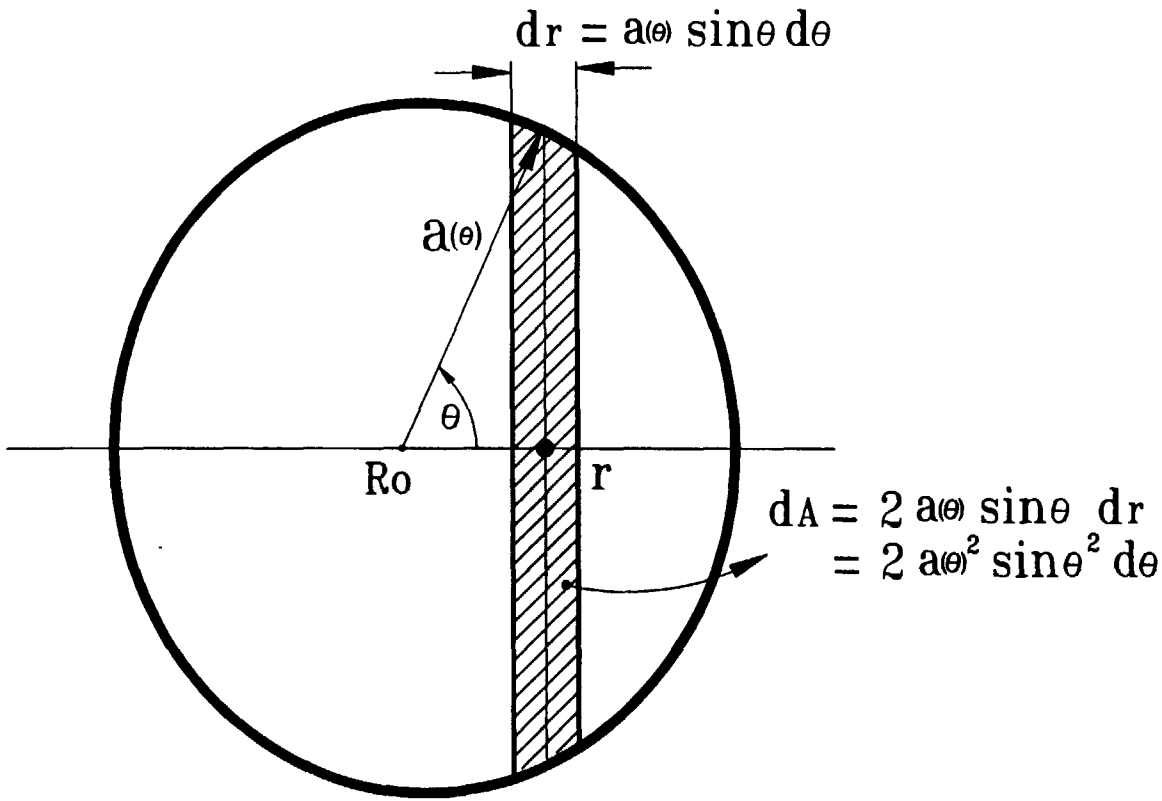

Fig.3. Model for surface integration over the vessel cross-section.

0.002845.

Evolution of the vessel eddy currents during toroidal coil charge for three values of the wall thickness is shown in Fig. 4. The currents increase abruptly from zero to the maximums in short times, order of τ_v's, and the profiles are very similar to simple exponential decays after the maximums.

The pressure acting on the vessel during field rise is produced by interaction of a basically decreasing current with a increasing field, therefore, there must be a maximum in the pressure profile as described in Fig. 5. The peak pressure depends on the wall thickness linearly in approximation, while the peak time is nearly constant for different thicknesses, determined by only the time constant of the coil, and is found around $2(\approx 2.86\ln 2)$ sec, when each of the current and the field has a half of it's maximum. For reference, relative errors of Equations (11), (11)', (12) and (12)' compared with the exact solution, Equation (8), are shown in Fig. 6.

During coil discharge both the current(as described in Fig. 4 considering only the trend) and the field decrease at $t>0^+$(~a few τ_v), then the maximum pressure appears at $t=0^+$(as indicated in Fig. 7) and is given by combination of the maimum current and the maximum field. The peak value is, as mentioned above, nearly $4/\alpha^2$ times higher than in the coil charge for the same wall thickness.

The pressure is inversely proportional to r^2, which may produces great unbalance in the spatial distribution of the pressure. The ratio, κ, of a maimum to a minimum in the pressure distribution is expressed as $\kappa=((A-1)/(A+1))^2$, here A is an effective aspect ratio. Because KT-2 is a large-aspect-ratio device, the unbalance factor κ is not so large and is about 3.3 as illustrated in Figures 8 and 9 showing the spatial distributions of the maximum pressure acting on the vessel during coil charge and discharge, respectively. The pressures are expressed as $-22500/r^2$(inward) and $+38690/r^2$(outward) during the charging and discharging stages, respectively, for 12 mm thick wall.

III. Diamagnetism change in a plasma disruption[6,7,8]

As the plasma looses it's energy due to some instabilities, the plasma temperature and the poloidal beta(β_p) decrease steeply in a very short time of a few hundreds μsec followed by the main disruption. Although the real loss mechanism of the plasma energy is not well known, it is reasonable to consider the energy to be lost linearly during the full period.

The pressure-balance equation in the plasma which has a large aspect ratio($R_p/a_p>>1$, a_p

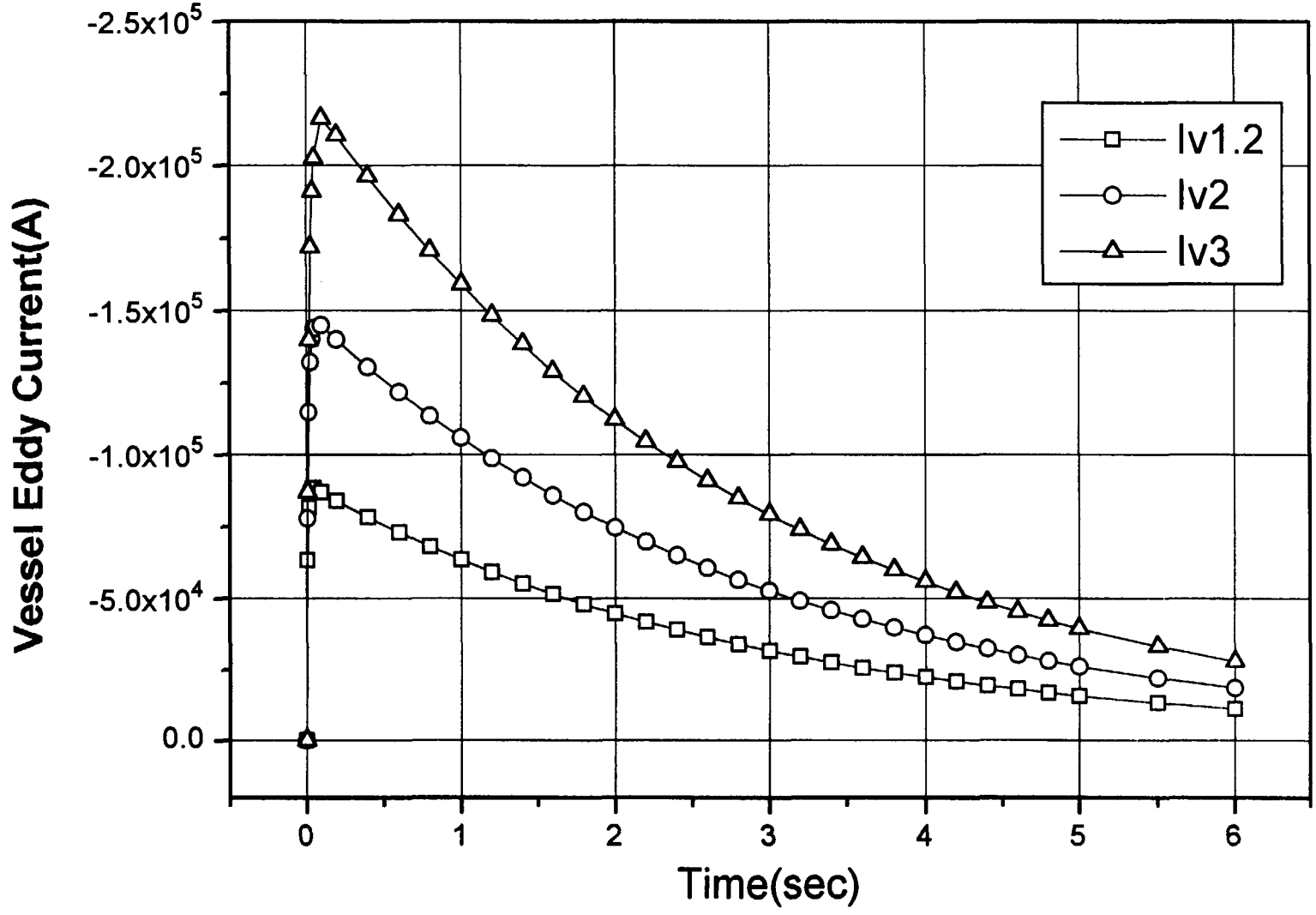

Fig. 4. Vessel currents induced during coil charge for three wall thicknesses(1.2,2 and 3 cm).

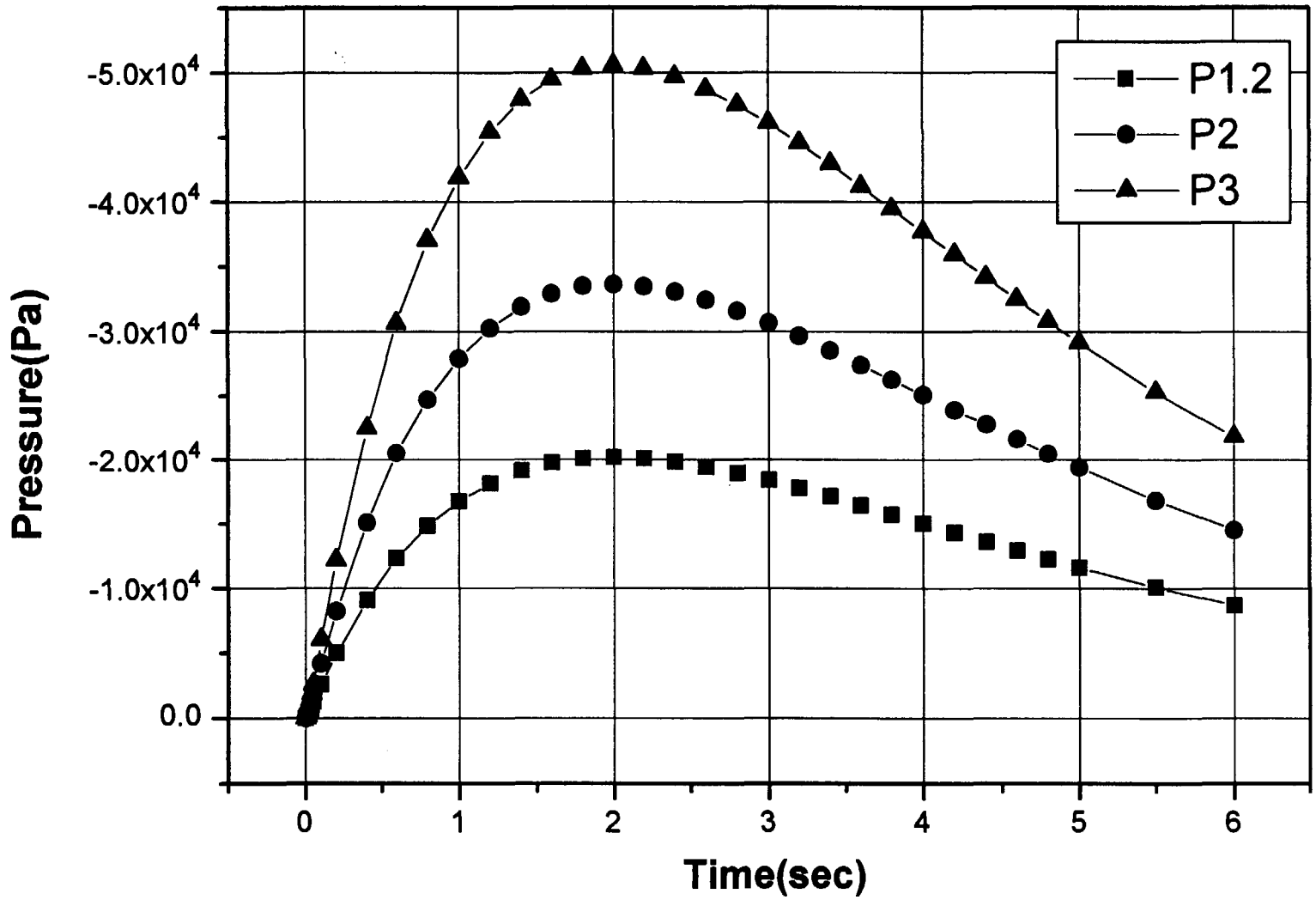

Fig. 5. Pressures acting on the vessel during coil charge for three wall thicknesses.

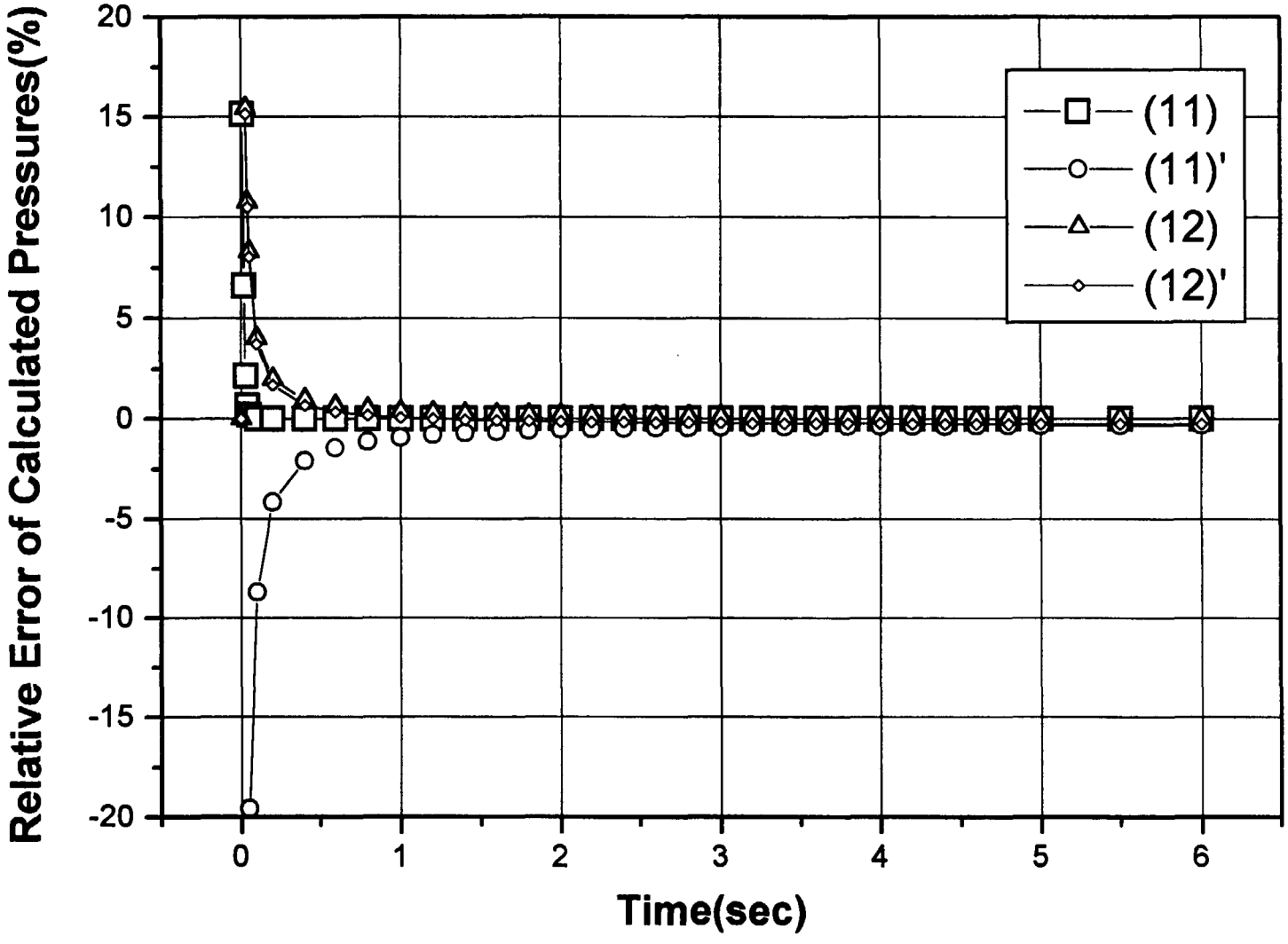

Fig. 6. Relative error of pressures calculated using approximate expressions(Eqs.11,11',12 and 12')

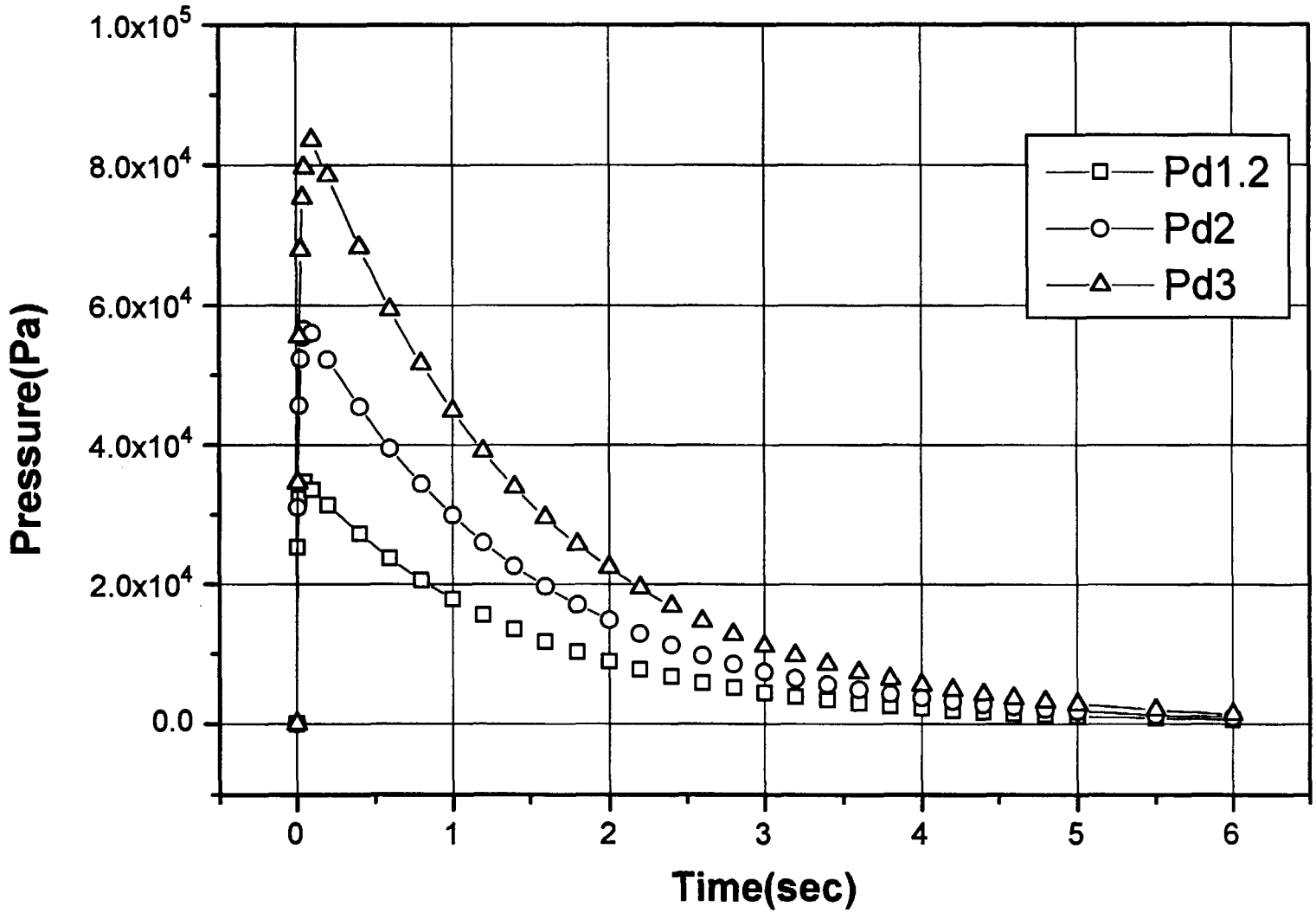

Fig. 7. Pressures acting on the vessel during coil discharge for three wall thicknesses.

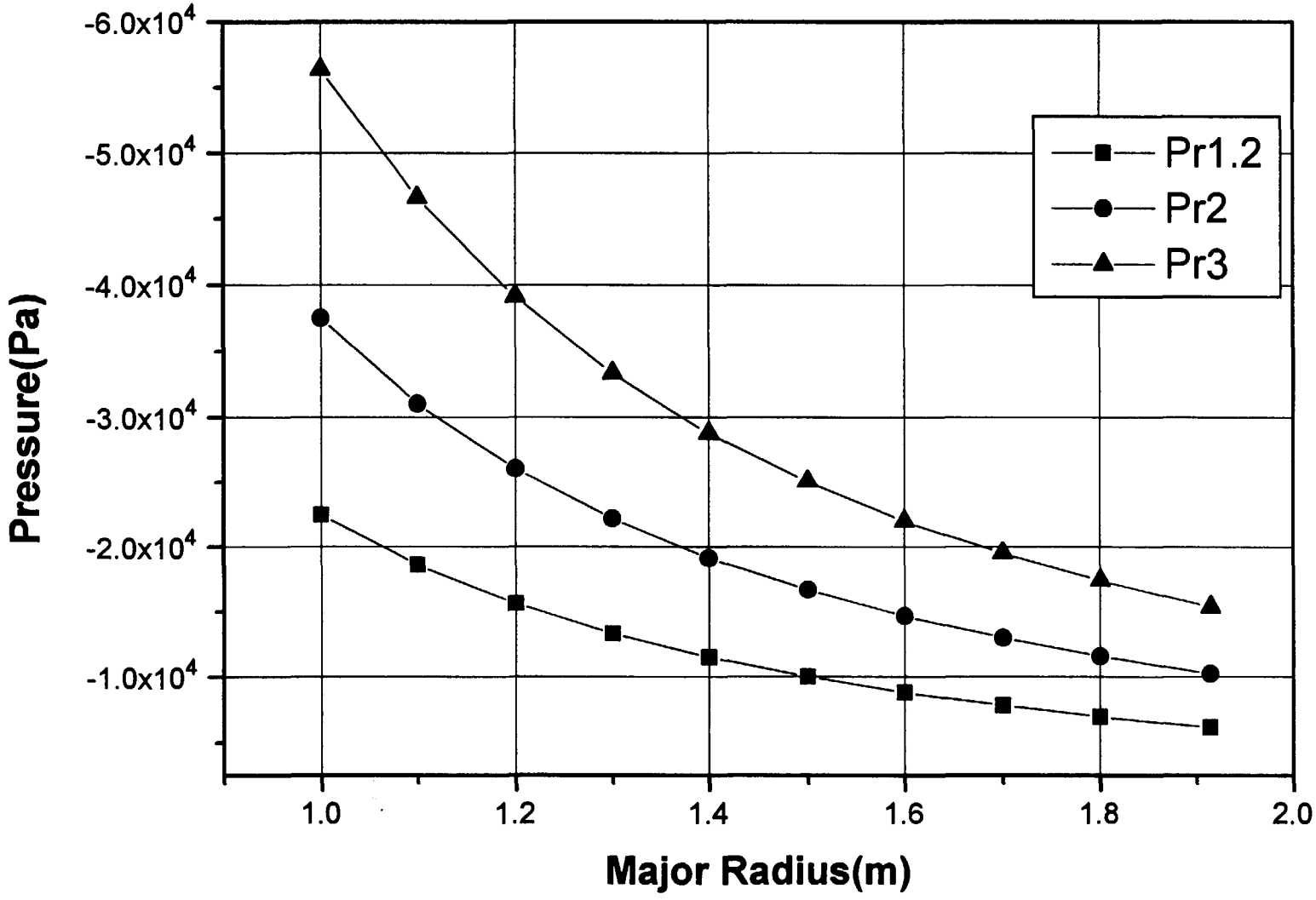

Fig. 8. Spatial variation of the maximum pressures acting on the vessel during coil charge.

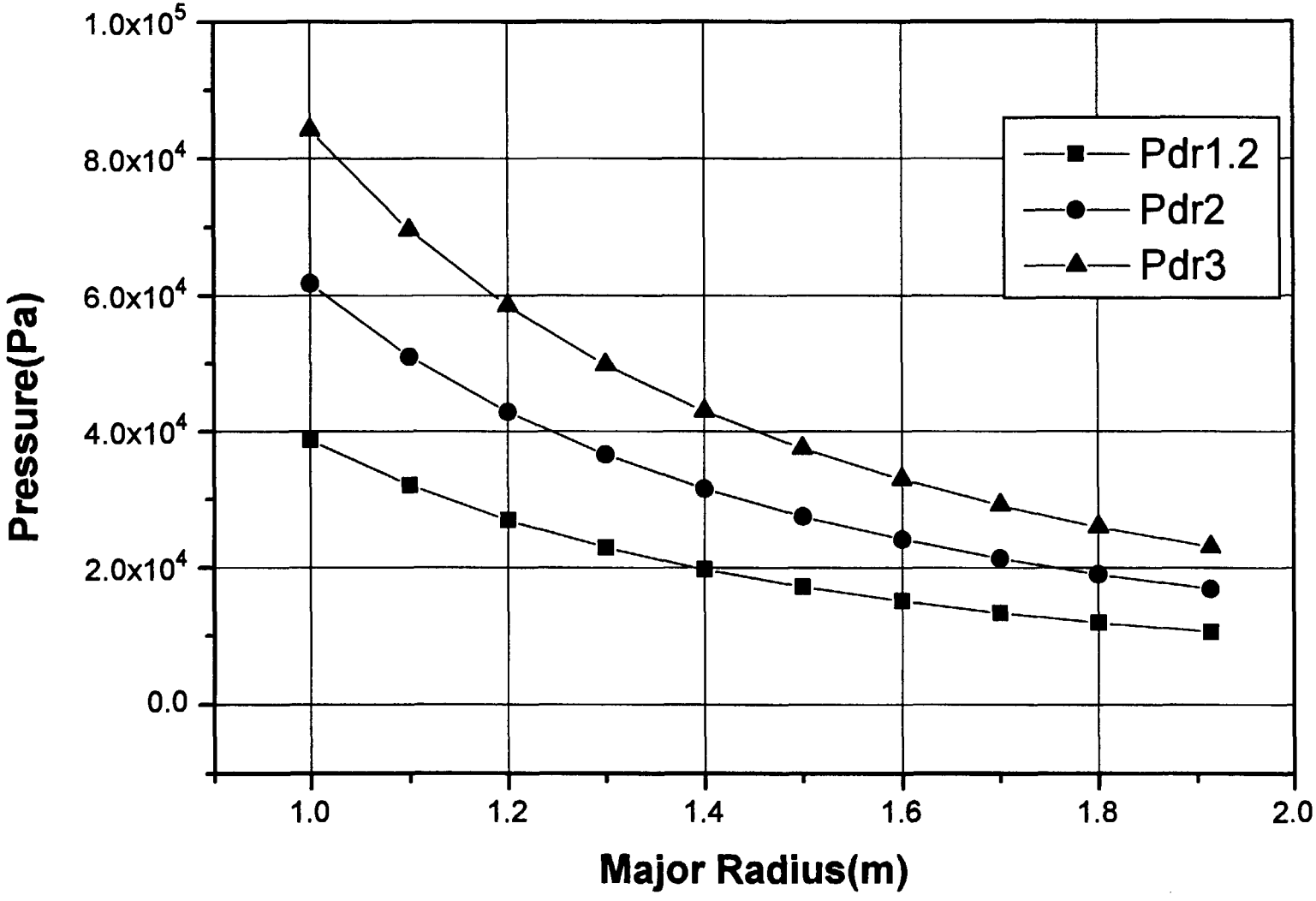

Fig. 9. Spatial variation of the maximum pressures acting on the vessel during coil discharge.

is the plasma minor radius) is written approximately in the following form.

$$<p> \cong \frac{<<B_p>>_\psi^2}{2\mu_0} - \frac{<B_t^2-B_{ta}^2>}{2\mu_0} \quad (18)$$

where, p: plasma pressure($=\Sigma n_k T_k$, n and T are density and temperature of kth species)[Pa]

$<\ >$: average over the volume containing the plasma, equivalent to the average over the plasma cross-section assuming axisymmetry.

$<<\ >>_\psi$: average over the flux surface, equivalent to the average along the perimeter of the plasma cross-section assuming axisymmetry.

$<<B_p>>_\psi = \int \mathbf{B}\cdot d\ell / \int d\ell = \mu_0 I_p / \int d\ell$, I_p is plasma current, $\int d\ell$ is a line integral along the plasma periphery($\approx 2\pi a_0((1+k^2)/2)^{1/2}$), a_0 and k are the short minor radius and elongation of the plasma cross-section.

B_{ta}: toroidal field in air or vacuum.

B_t inside the plasma is produced by internal poloidal current source as well as external toroidal field coils, while B_p is produced by the toroidal plasma current. For given plasma current and the plasma pressure profiles, $<B_t^2-B_{ta}^2>$ is adjusted in such a way that the pressure-balance equation is satisfied. If we define $\Delta\Phi$ as flux change due to plasma diamagnetism or paramagnetism, then $\Delta\Phi = \int (B_t-B_{ta})ds \equiv <<B_t-B_{ta}>>_S$ where s denotes the plasma cross-section. As $<B_t^2-B_{ta}^2> = <(B_t+B_{ta})(B_t-B_{ta})> \approx 2<B_{ta}(B_t-B_{ta})> = 2\pi R_p B_{t0} <<B_t-B_{ta}>>_S /V \approx 2B_{t0}\Delta\Phi/S$, where V is the volume of the plasma and S is the area of the plasma cross-section($S \approx \pi a_0^2 k(2J_1(\delta)/\delta)$, $J_1(x)$ is the first order Bessel function of the first kind and δ is triangularity of the plasma cross-section, $V = 2\pi R_p(1-0.233\delta/A)S \cong 2\pi R_p S$), Equation (18) is arranged as Equation (19).

$$\Delta\Phi = \frac{\mu_0^2 I_p^2}{8\pi B_{t0}} \frac{(4kJ_1(\delta)/\delta)}{(1+k^2)} (1-\beta_p) \quad (19)$$

where, β_p: average poloidal beta($=2\mu_0<p>/<<B_p>>^2$;plasma kinetic energy÷magnetic energy)

$\Delta\Phi > 0$ if $\beta_p < 1$(paramagnetic; increase of toroidal magnetic field), and $\Delta\Phi < 0$ if $\beta_p > 1$ (diamagnetic; decrease of toroidal magnetic field) as illustrated in Fig. 10.

In the totoidal device there exists always a toroidal magnetic field. Without plasma there is no change of the toroidal magnetic flux($\Delta\Phi = 0$). As plasma is generated (possibly by RF)

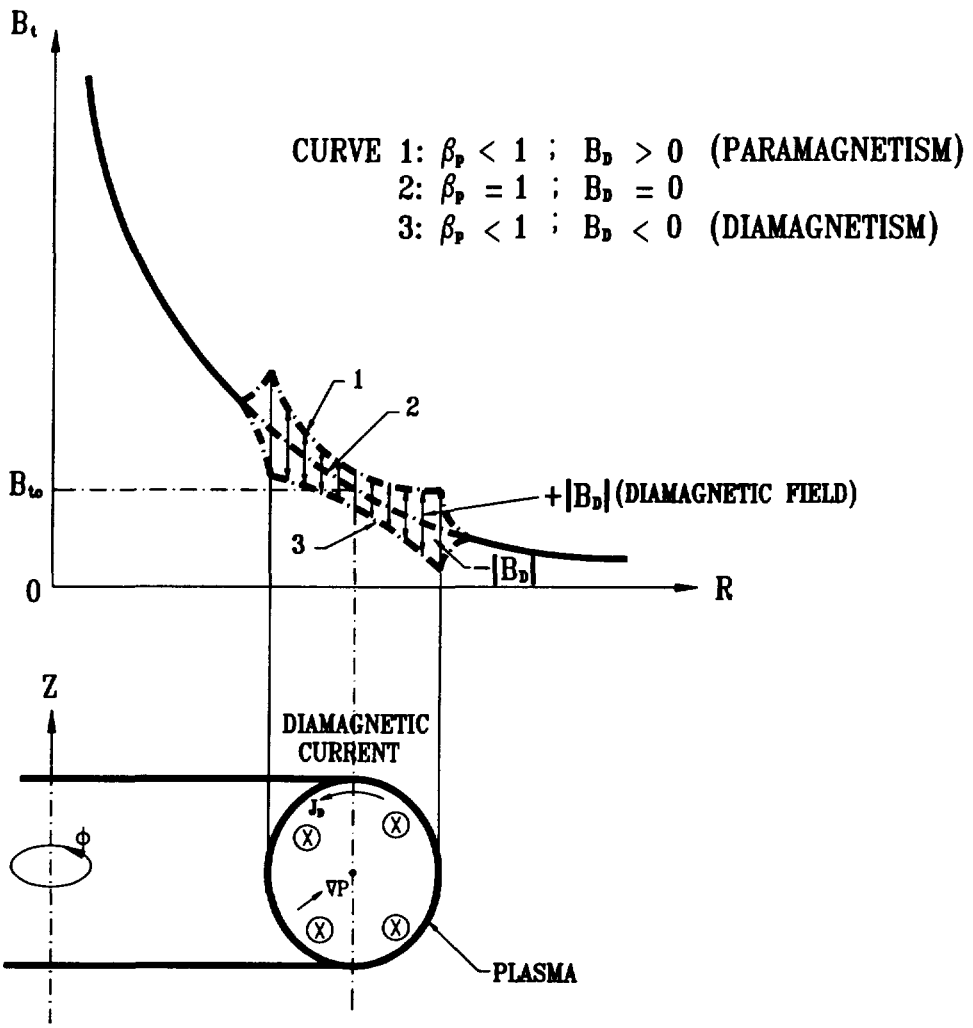

Fig.10. Diamagnetism change in the tokamak plasma.

in the magnetic field, diamagnetic current induced by the radial gradient of the plasma pressure starts to flow and produces additional toroidal fields antiparallel to the original one, which represents there may be abrupt change of the toroidal flux. If the plasma is initiated by a toroidal loop voltage there must be a toroidal current producing poloidal magnetic fields whose radial gradient can make paramagnetic poloidal current. In a cold plasma($\beta_p \approx 0$), as just genrated before sufficient heating, paramagnetic current is larger than diamagnetic one, and $\Delta\Phi > 0$, but the magnitude is expected to be small because of low plasma current.

As the plasma (toroidal) current develops further, flux change depends only on the current, that is $\Delta\Phi \sim I_p^2$. If the plasma is heated up sufficiently by RF or NBI the diamagnetic current increases and takes over the paramagnetic one, the net change of $\Delta\Phi$ is negative ($\beta_p > 1 \rightarrow \Delta\Phi < 0$).

In the plasma disruption the current quench, relatively slow phenamenon, follows the energy quench[9]. During the energy quench the plasma current is assumed to be not changed, but the poloidal beta decreases to zero, which causes increase of $\Delta\Phi$, while during the current quench the plasma current decays to zero, which results in decrease of $\Delta\Phi$. Current ramp down in the end of a normal mode may cause an increase of the poloidal beta, which make the flux change complicate, but it is not easy to treat it theoretically here. Figure 11 shows typical relation of the variations of the plasma curent, diamagnetic signal and poloidal beta[7].

When the plasma poloidal beta changes from β_{pi} to β_{pf} in Δt_e, the vessel current induced during a plasma disruption, I_v, is given by following equation.

$$I_v = -\frac{\delta\Phi}{R_v \Delta t_e}(1 - e^{t/\tau_v}) \simeq -\frac{\delta\Phi\,\tau_v}{L_v \Delta t_e}(1 - e^{t/\tau_v}) \qquad (20)$$

where, $\delta\Phi = \Delta\Phi_f - \Delta\Phi_i$, suffix i and f denote initial and final values, $\Delta\Phi_f = xx(1-\beta_{pf})$, $\Delta\Phi_i = xx(1-\beta_{pi})$, finally $\delta\Phi = xx(\beta_{pi}-\beta_{pf})$(refer to Equation (19) for the exact expression of the term xx).

If $\Delta\Phi$ is non-zero during Δt_e and assuming $\Delta t_e << \tau_v$, the maximum vessel current I_{vm} is approximately given by $\delta\Phi/L_v$. This means that flux change is almost converted to magnetic energy of the vessel rather than resistive consumption during Δt_e. And note that I_v has minus sign if $\beta_{pi} > \beta_{pf}$, and vice versa. Then using Equations (1), (19) and (20) the pressure is expressed as Equation (21).

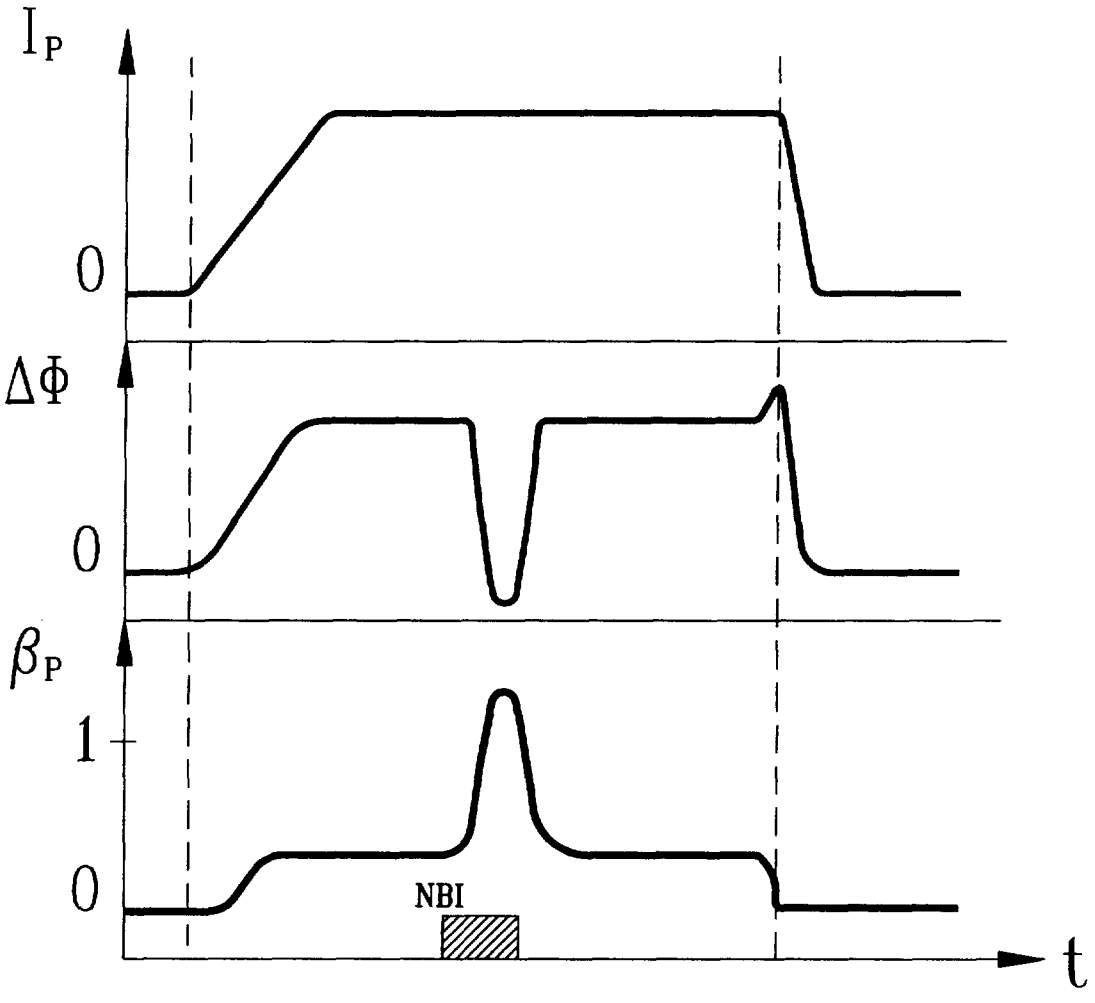

Fig.11. Variations of the plasma current, diamagnetism and poloidal beta.

$$P = -\frac{\delta\Phi}{2\pi r L_v}\left(\frac{B_{to}R_p}{r} + \frac{\mu_0\delta\Phi}{4\pi r L_v}\right)$$

$$= -\frac{\mu_0^2 I_p^2(\beta_{pi}-\beta_{pf})\lambda R_p}{16\pi^2 L_v r^2} + \frac{\mu_0^5 I_p^4(\beta_{pi}-\beta_{pf})^2\lambda^2}{256\pi^4 B_{t0}^2 L_v^2 r^2} \qquad (21)$$

where, $\lambda = 4kJ_1(\delta)/\delta(1+k^2)$

The second term of RHS of Equation (21) is much less than the first term, it is, therefore, neglected in the sample calculation using the parameters of KT-2 which is summarized in Table 2.

$\delta\Phi$ is calculated during the plasma disruption for β_{pi}=2.3 to be 9.77x10^{-3} Wb, assuming β_{pf} is reasonably 0, and I_{vm} is -7.325x10^4 A. Then the pressure acting on the vacuum vessel is expressed as -48965/r^2, which implies the inward pressure.

If β_p is nearly zero or constant and there is only a linear change of the plasma current I_p as $I_p(t)=I_i+(I_f-I_i)t/\Delta t_k=I_i+\gamma t$(k=r for current rising, k=c for current quench, I_i is the initial current, γ is the change rate of the plasma current), I_v and P are given as below.

$$I_v = -\frac{2Q}{R_v}\gamma((I_i - \gamma\tau_v)(1 - e^{-t/\tau_v}) + \gamma t) \qquad (22)$$

$$P = -\frac{2Q}{R_v}\frac{B_{to}R_p}{2\pi r^2}\gamma((I_i - \gamma\tau_v)(1 - e^{-t/\tau_v}) + \gamma t) \qquad (23)$$

where, $Q=\mu_0^2\lambda(1-\beta_p)/8\pi B_{t0}$.

If $\gamma>0$ (during plasma initiation), it is easily found that I_v increases monotonically, then we can obtain approximate forms of Equation (22) as follows;

for $t<<\tau_v$

$$I_v \approx -\frac{2Q\gamma(I_i+\gamma t/2)}{L_v}t \qquad (24)$$

and for $t>>\tau_v$

$$I_v \approx -\frac{2Q\gamma^2}{R_v}t = -\frac{2Q\gamma}{R_v}I_p \qquad (25)$$

If $\gamma < 0$ (during plasma disruption), there is a maximum in I_v and P at $t = \tau_v \ln(1 - I_i/\gamma\tau_v)$, as given by Equations (26) and (27).

$$I_v = -\frac{2Q\gamma}{R_v}(I_i + \gamma\tau_v \ln(1 - I_i/\gamma\tau_v)) \tag{26}$$

$$P = -\frac{2Q\gamma}{R_v}\frac{B_{to}R_p}{2\pi r^2}(I_i + \gamma\tau_v \ln(1 - I_i/\gamma\tau_v)) \tag{27}$$

For two extreme cases 1) $I_i/\gamma << \tau_v$ and 2) $I_i/\gamma >> \tau_v$, Equation (26) may be approximated to following equations.

1) $$I_v \approx \frac{Q I_i^2}{L_v} \tag{28}$$

2) $$I_v \approx -\frac{2Q\gamma}{R_v} I_i \tag{29}$$

Equation (28) can be also derived by the relation $\Delta I_v = \Delta\Phi/L_v = QI_i^2/L_v$ (when I_p changes from I_i to 0). Equation (29) is basically equivalent to Equation (25).

Using the parameters of Table 2 and assuming $\gamma = 1$ MA/s in the start-up, $\gamma = -500$ MA/s in the disruption, and $\beta_p = 0$ in the both stages, variations of the vessel current are described as Fig. (12) and Fig. (13), respectively. Maximum induced vessel currents are calculated to be -1019 A during current rise in Equation (22), and 29448 A during current quench in Equation (26). The pressure exerting on the vessel due to diamagnetism change by current rise and current quench during the plasma initiation and disruption are expressed as $-682/r^2$ and $19684/r^2$, respectively. Table 3 summarizes whole results obtained above.

The non-uniform spatial distribution of the pressure and the toroidal geometry of the tokamak vessel leads to non-vanishing horizontal forces exerting on the vessel. The pressures obtained above all have the form of P_0/r^2 ($P_0 \approx I_v B_{to} R_p/2\pi$). Horizontal force(centering or expanding) is obtained by integration of the radial component of the normal pressure as illustrated by Equation (30).

$$F_r = \int 2\pi r P\cos\theta \, d\ell = \int 2\pi r P\cos\theta \, a\, d\theta = 2\pi \int P r dz = 2\pi P_0 \int dz/r \tag{30}$$

If any functional expression for the plasma boundary is given, F_r is calculated analytically or

Table 2. Plasma paremeters related with the plasma beta change.

I_p	500 kA
R_p	1.4 m
a_0	0.5 m
A	5.6
k	1.8
δ	0.6
$J_1(\delta)$	0.2867
$\lambda (=4kJ_1(\delta)/\delta(1+k^2))$	0.8114
β_p	2.3
β_p/A	0.45
$Q(=\mu_0^2 \lambda (1-\beta_p)/8\pi B_{t0})$	$1.7 \times 10^{-14}(\beta_p=0)$
Δt_e(energy quench)	~0.5 ms
Δt_c(current quench)	~1 ms
Δt_r(current rising)	0.5 s

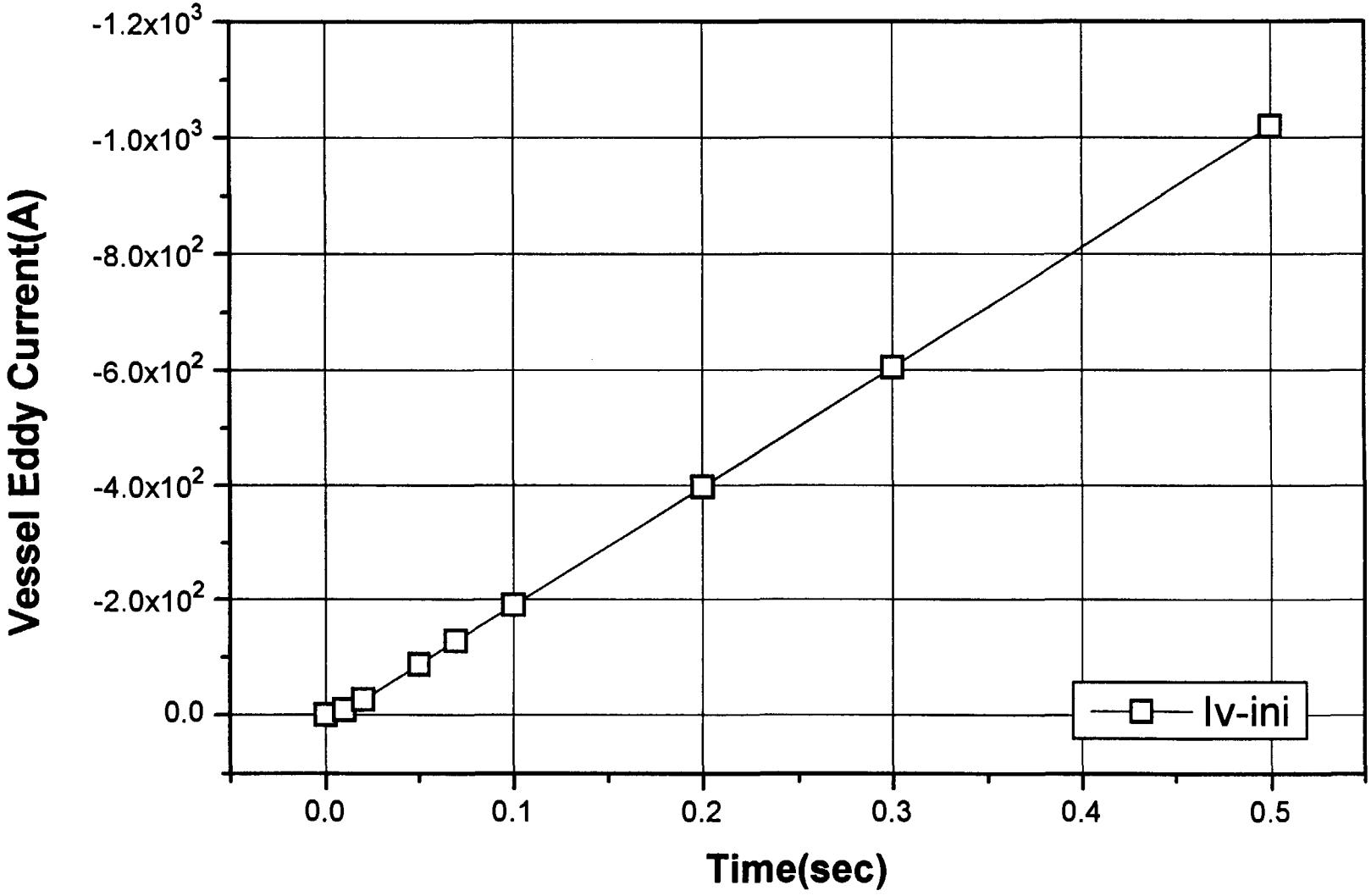

Fig.12. Variation of the vessel current induced by diamagnetism change during plasma initiation.

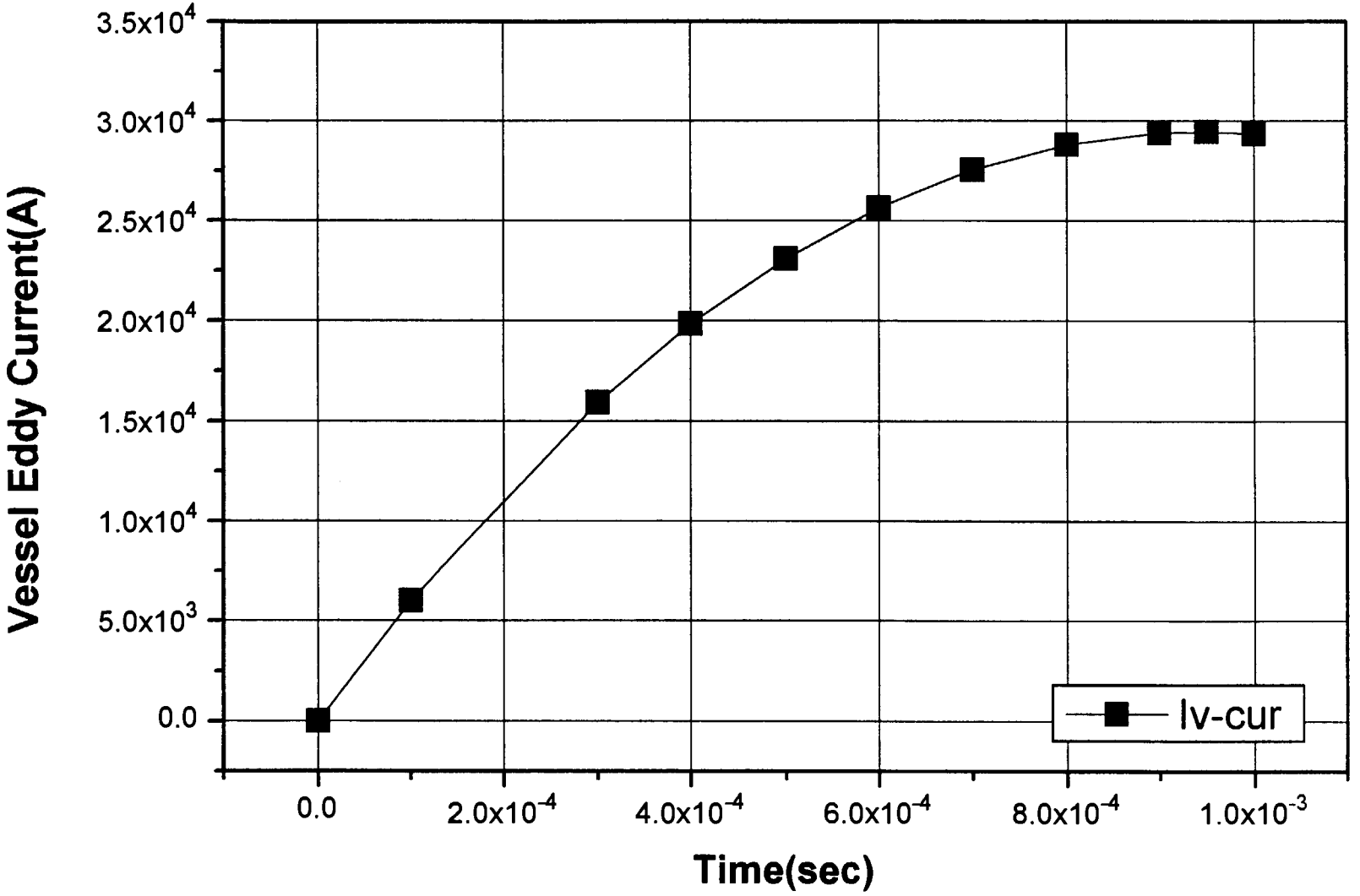

Fig.13. Variation of the vessel current induced by diamagnetism change due to current quench.

Table 3. The pressures induced on the vessel during toroidal field changes.

TF change	
-TF rising	$-22498/r^2$ Pa
-TF damping	$+38687/r^2$ Pa
Diamagnetism	
-energy quench during disruption	
$\beta_p = 2.3$	$-48965/r^2$ Pa
$\beta_p = 0$	$+21289/r^2$ Pa
-plasma current change(β_p=0)	
· current rising dI_p/dt = +1MA/s	$-682/r^2$ Pa
· current decay in disruption dI_p/dt = -500MA/s	$+19684/r^2$ Pa

numerically. For the KT-2 vacuum vessel(refer to Fig. 2) we get following equation.

$$F_r = 4\pi P_0\left(\int_0^{\varepsilon}\frac{a_1\cos\theta\,d\theta}{R_1+a_1\cos\theta}+\int_{\varepsilon}^{\pi}\frac{a_2\cos\theta\,d\theta}{R_2+a_2\cos\theta}+\frac{z_2}{(R_2-a_2)}\right)$$

$$= 4\pi P_0\left(\left(\theta-\frac{2R_1}{\sqrt{(R_1^2-a_1^2)}}\tan^{-1}\frac{((R_1-a_1)\tan\theta/2)}{\sqrt{(R_1^2-a_1^2)}}\right)\Big|_0^{\varepsilon}+\right.$$

$$\left.\left(\theta-\frac{2R_2}{\sqrt{(R_2^2-a_2^2)}}\tan^{-1}\frac{((R_2-a_2)\tan\theta/2)}{\sqrt{(R_2^2-a_2^2)}}\right)\Big|_{\varepsilon}^{\pi}-z_2/(R_2-a_2)\right) \qquad (31)$$

Using the parameters given at Table 1, $F_r = -3.05P_0$, which indicates that an inward pressure produces a net force directing the large major radius side, and vice versa (contrary to the trend for atmospheric pressure of uniform distribution). An approximate form of the radial force is obtained from Equation (30). That is, $F_r=2\pi P_0\int dz/r=2\pi P_0\int rdz/r^2\approx 2\pi P_0\int dA/R_0^2=2\pi P_0A_v/R_0^2$($A_v$ is the cross-sectional area of the vessel).

We can also get an expression for vertical force F_v as follows;

$$F_v = 2\pi P_0\left(\int_0^{\varepsilon}\frac{a_1\sin\theta\,d\theta}{R_1+a_1\cos\theta}+\int_{\varepsilon}^{\pi}\frac{a_2\sin\theta\,d\theta}{R_2+a_2\cos\theta}\right)$$

$$= -2\pi P_0\left(\ln(R_1+a_1\cos\theta)\Big|_0^{\varepsilon}+\ln(R_2+a_2\cos\theta)\Big|_{\varepsilon}^{\pi}\right) \qquad (32)$$

As inserting KT-2 parameters to Equation (32), the relation $F_v = +3.96P_0$ is obtained. Table 4 summaries the horizontal and vertical forces acting on the KT-2 vessel for the three modes producing the pressures of $1/r^2$ form.

Ⅳ. Stress Analysis

The functional forms of the pressure acting on the vacuum vessel due to the poloidal eddy currents in any operation modes disussed above have the characteristic term of $1/r^2$. It is easily expected that similar patterns will be obtained in the stress distribution if it is caused by the forces of the same spatial variation. Therefore, stress analysis was performed for only

Table 4. The forces exerting on the vessel during toroidal field changes.

TF rising	F_r +68691 Nt (centrifugal) F_v -88998 Nt (compression)
TF damping	F_r -118119 Nt (centripetal) F_v +153038 Nt (tension)
Diamagnetism	
$\beta p = 2.3$	F_r +149342 Nt F_v -193900 Nt
$\beta p = 0$	F_r -64931 Nt F_v +84304 Nt
dI_p/dt=1MA/s	F_r +2080 Nt F_v -2701 Nt
dI_p/dt=-500MA/s	F_r -60036 Nt F_v +77949 Nt

two modes of TF damping and energy quench considering directions and magnitudes of the pressure(refer to Table 3).

The stress analysis was performed using 3D FEM code (ANSYS 5.2). ANSYS code consists of three processors; General Processor(/PREP7)-model generation, Solution Processor (/Solu)-define boundary conditions and solve the problem, General PostProcessor(/POST1)-estimate analysis results.

Table 5 summaries the parameters used in the stress analysis. Fig. 14 is the 3D finite element model describing a quarter of the KT-2 vacuum vessel. This model includes all ports installed in the 90° section and one support. All weldments are asssumed to have the same material property with the original wall. It is also supposed that the vessel material is isotropic and elastic(Hooke's law is valid).

Figures 15 and 16 show 3D distributions of stress and deformation due to the atmospheric pressure applied uniformly on the vessel before tokamak discharge. The maximum stress appears at the boundary of the vessel wall and the NBI port to be 0.612×10^8 Pa. It may be, however, much different from an average stress pattern, which is easily guessed from the fact that cool-colored pattern of relatively low stress covers almost whole surface of the model and hot-colored area of high stress is extremely localized as shown in Fig. 15. The maximum deformation is 0.241 mm.

Figures 17 and 18 show the stress and deformation distributions on the vessel during TF damping. In this mode, the total mechanical load to the vessel is given as combination of the force due to TF damping itself and the atmospheric pressure. Because the induced pressure due to decrease of the toroidal field is outward which cancels much of the atmospheric pressure, the stress in this case is expected to moderate compared with the stress due to atmospheric pressure only. The majority of vacuum vessel has the stress in the range of $0.620 \times 10^7 \sim 0.248 \times 10^8$ Pa. The maximum stress is 0.558×10^8 Pa occurred at the welding line between the wall and the NBI port. This value is larger than 1/3 of the yield strength of s.s 304L, which means reinforcing structures must be added to the NBI port. The maximum deformation is 0.223 mm.

Fig. 19 is the stress distribution on the poloidal belt at a minor vessel cross-section far from the ports. This result is easily understandable and looks very reasonable comparing with 2D analysis(not shown here).

Figures 20 and 21 show 3D stress and deformation distributions due to diamagnetism change(increase of toroidal field) in the energy quench during a plasma distruption. Since the pressure caused by increase of the toroidal field is inward, then it adds to the atmospheric one. The stress on most part of vacuum vessel is in the range of $0.756 \times 10^7 \sim 0.302 \times 10^8$ Pa.

Table 5. Input parameters for the stress analysis.

Material	SUS304L , Isotropic
EMUNIT	MKS
ANTYPE	STATIC
Element Type	SHELL 63
Element Size	less than 3 cm
Element Numbers	15802 ea
Young's Modulus	1.88×10^{11} N/m^2
Density	7900 kg_m/m^3
Poisson's ratio	0.27
Real constant	
. small circle port wall thickness	5 mm
. slim port wall thickness	10 mm
. vacuum vessel wall thickness	12 mm
. big, NBI port wall thickness	15 mm
. small,slim,NBI port flange thickness	25 mm
. big port flange thickness	30 mm
Main coordinate system	Cylindrical
Theta ; $\theta = 0^\circ$, 90°	Symmetry (quarter modeling)
Constraint	
. $64^\circ < \theta < 71^\circ$, $-94.2^\circ < \varphi < -58.5^\circ$	All DOF

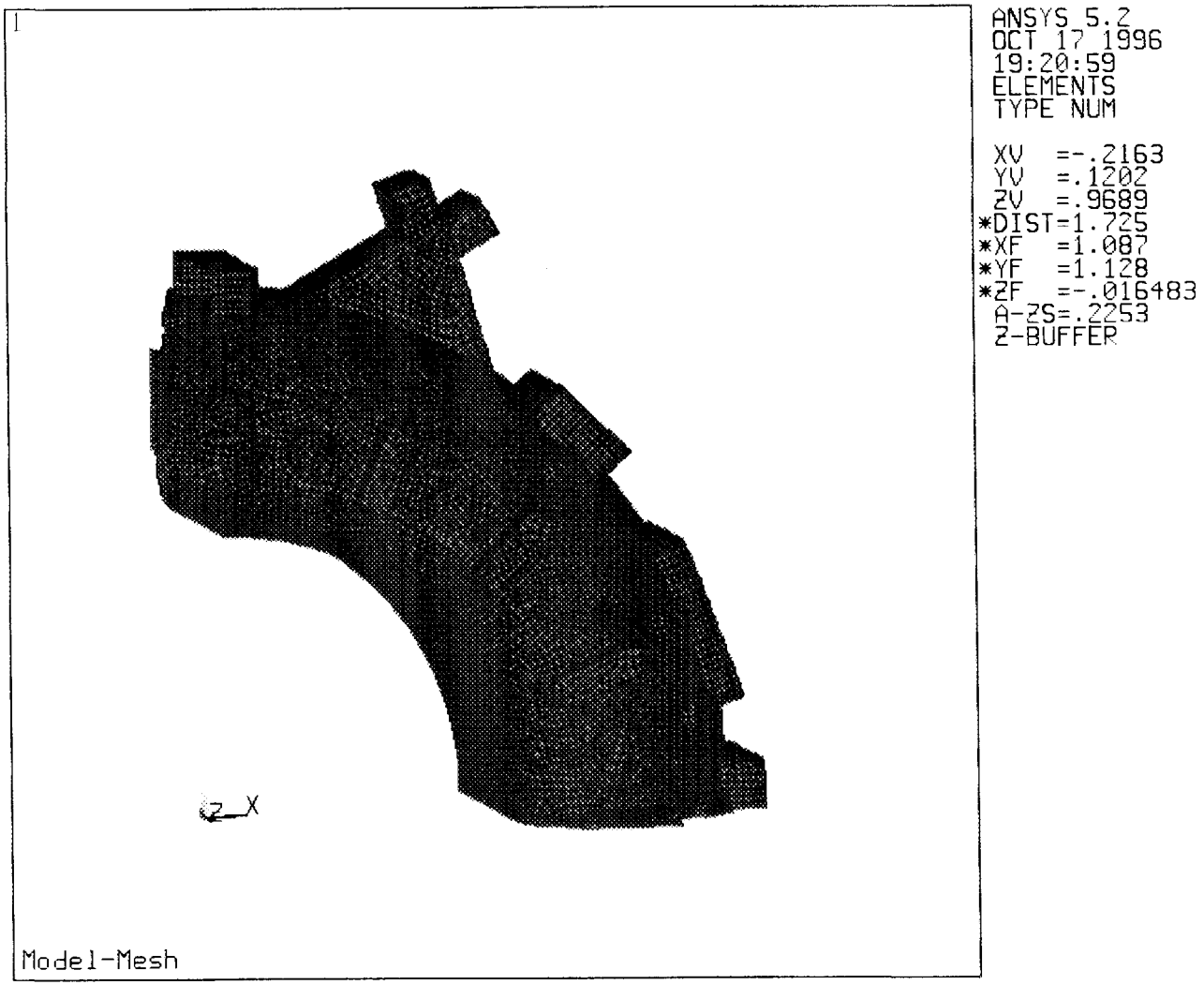

Fig. 14. 3D finite element Model of the KT-2 vacuum vessel.

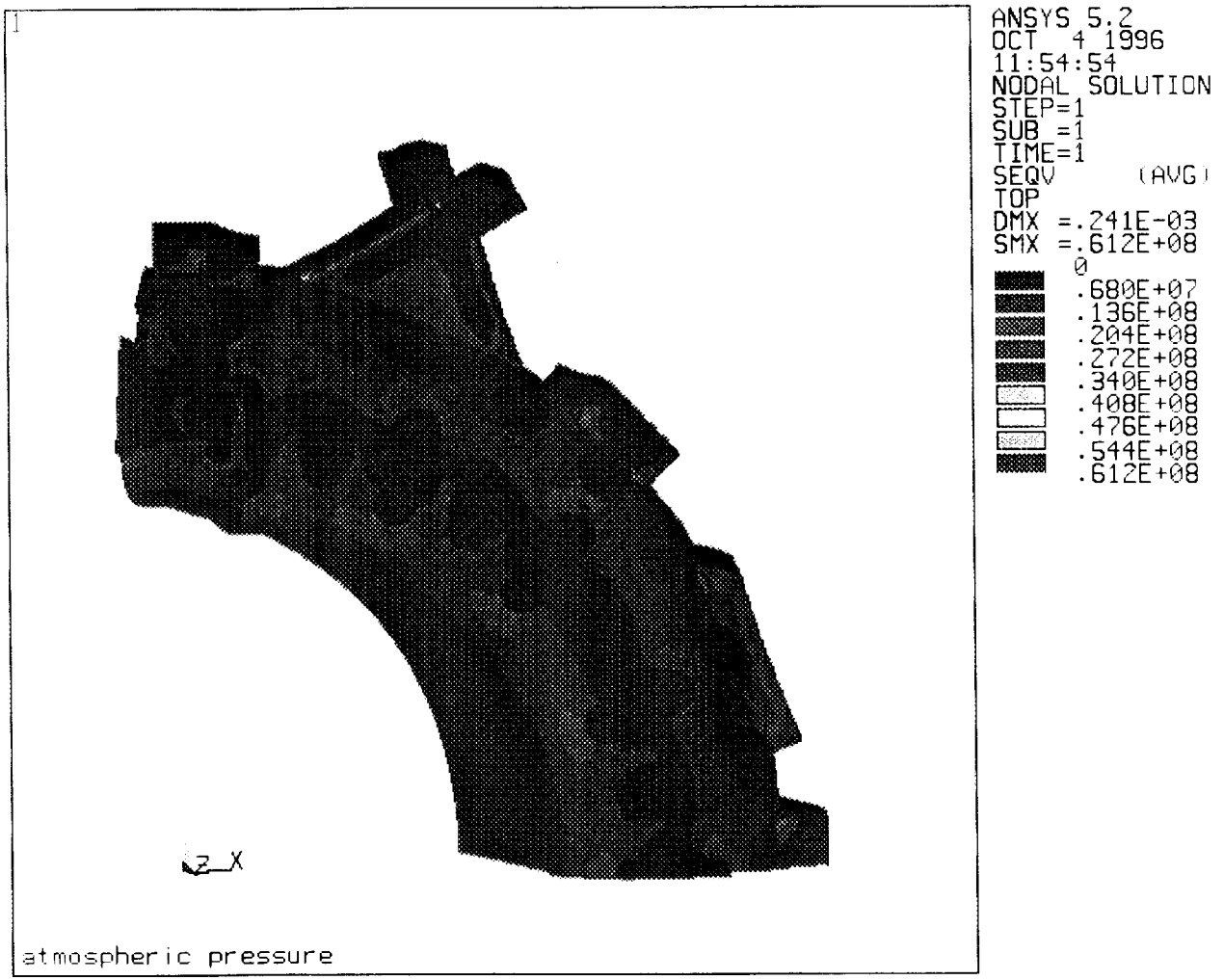

Fig. 15. Stress distribution on the vessel by the atmospheric pressure.

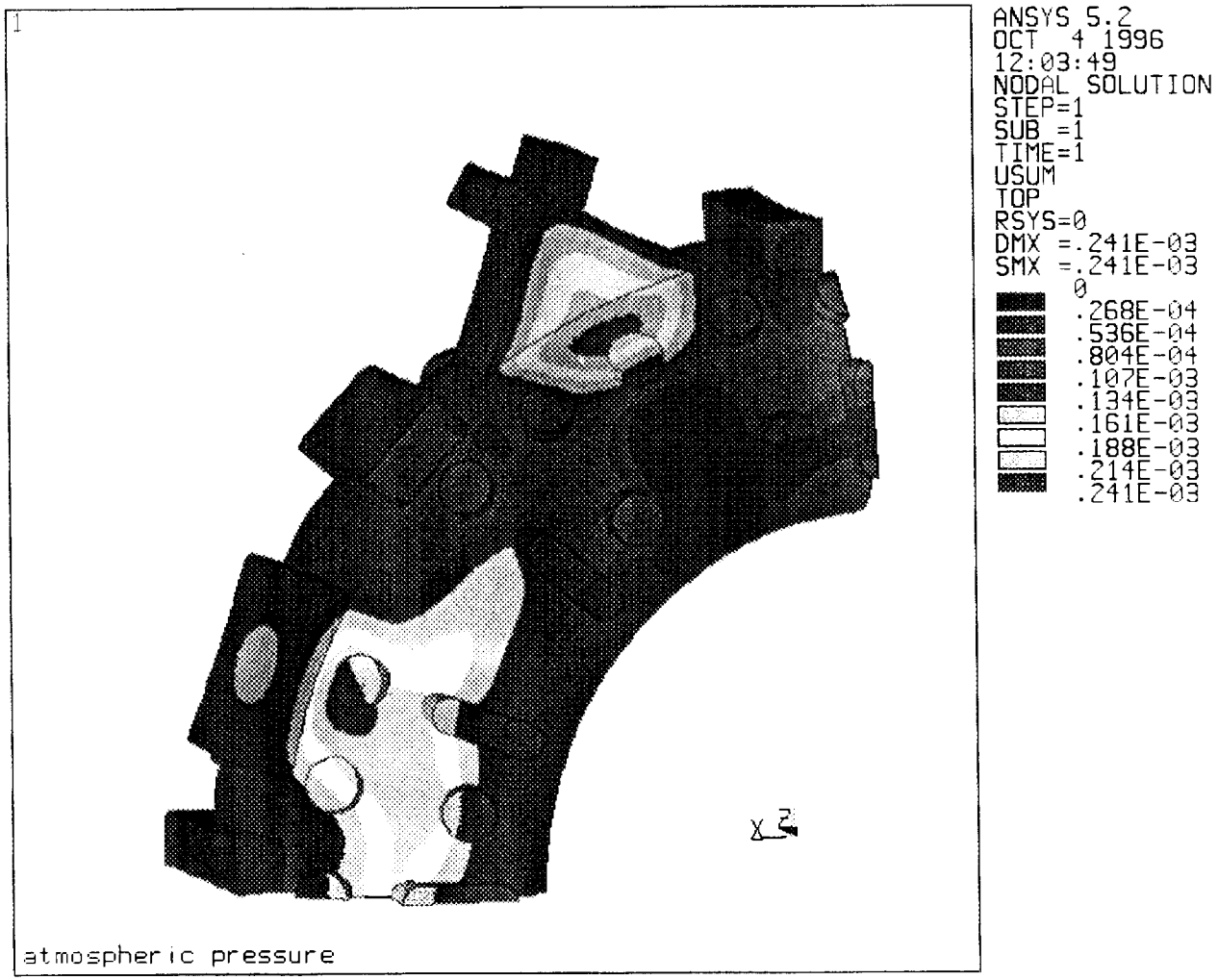

Fig. 16. Deformation of the vessel by the atmospheric pressure.

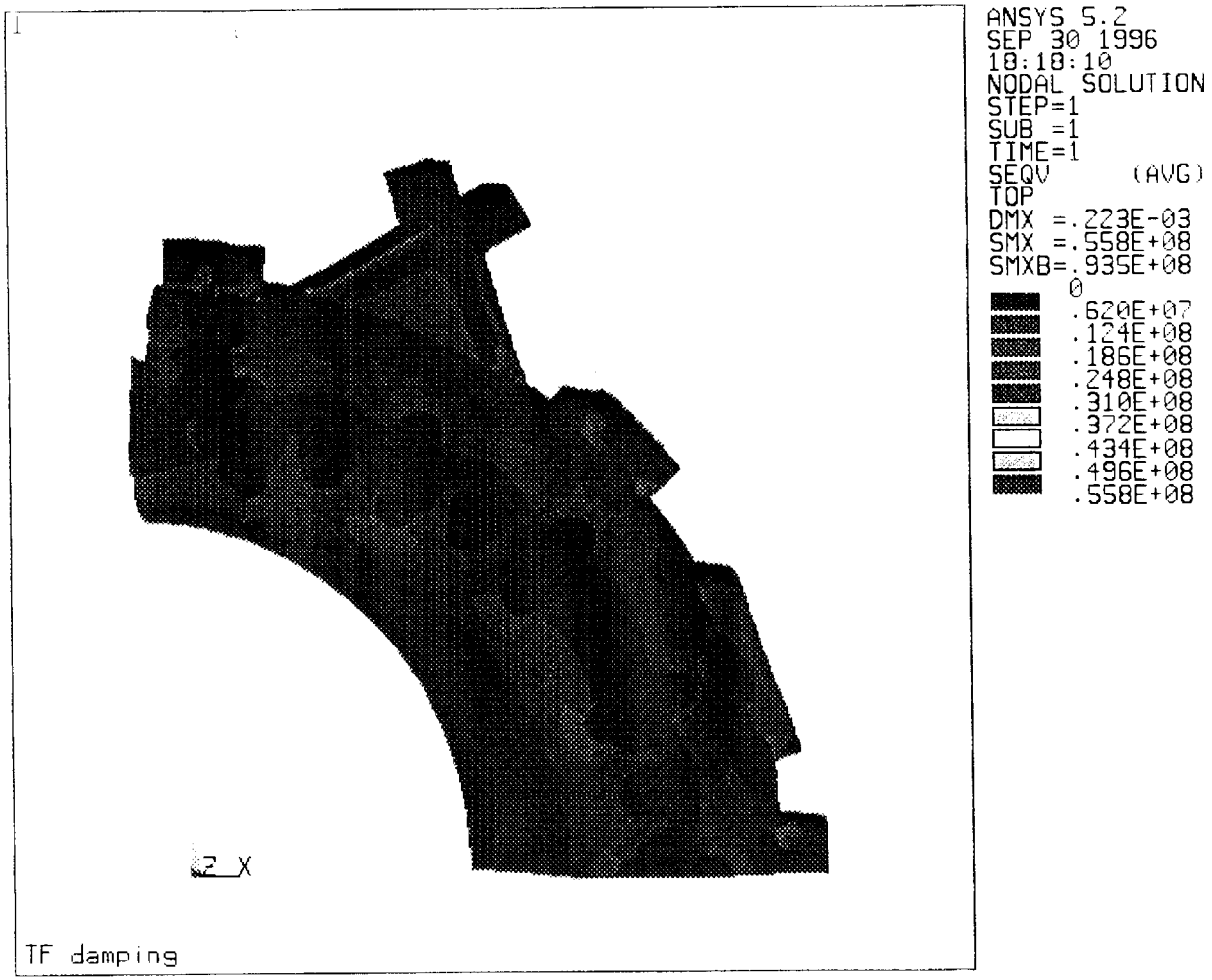

Fig. 17. Stress distribution on the vessel during TF damping.

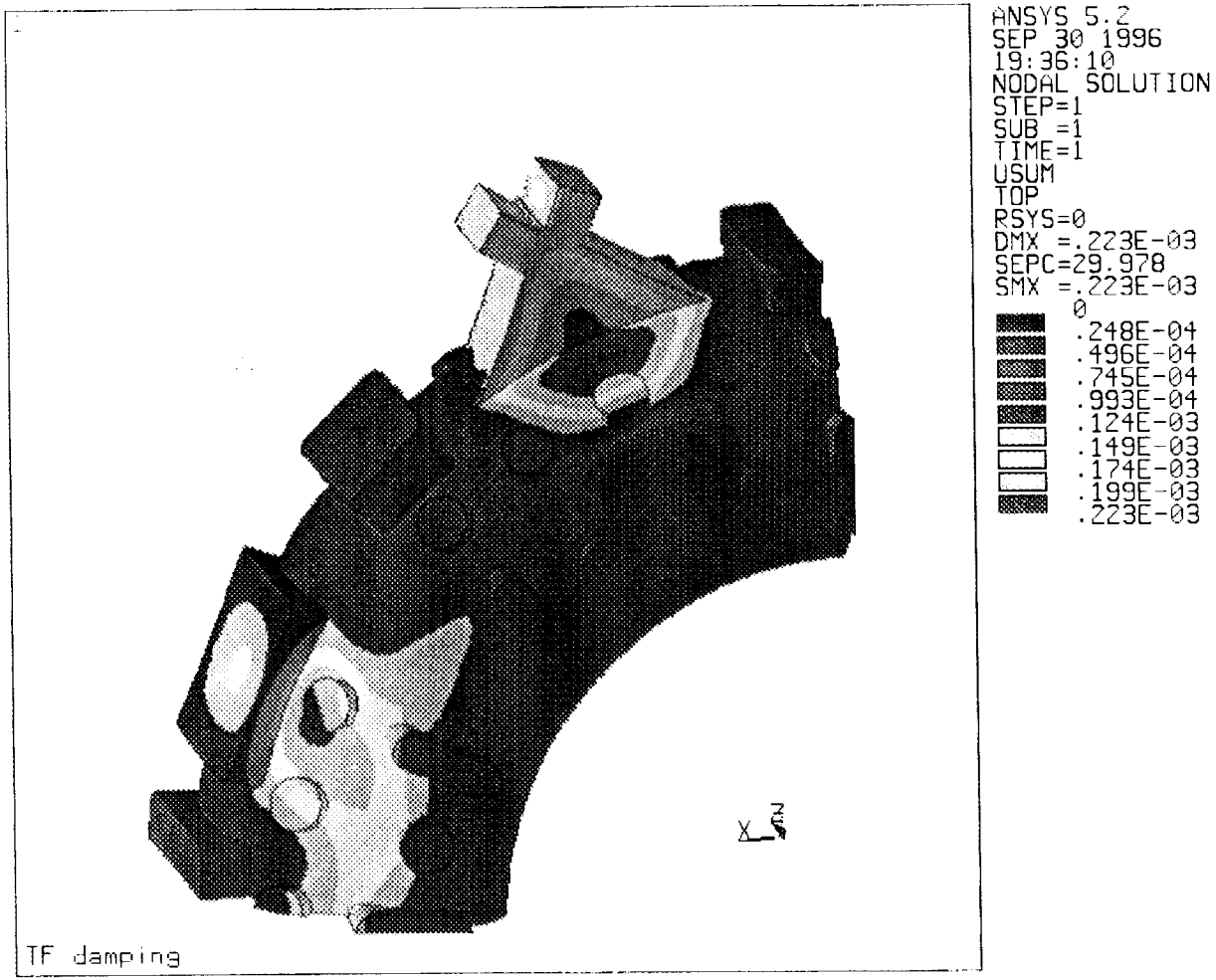

Fig. 18. Deformation of the vessel during TF damping.

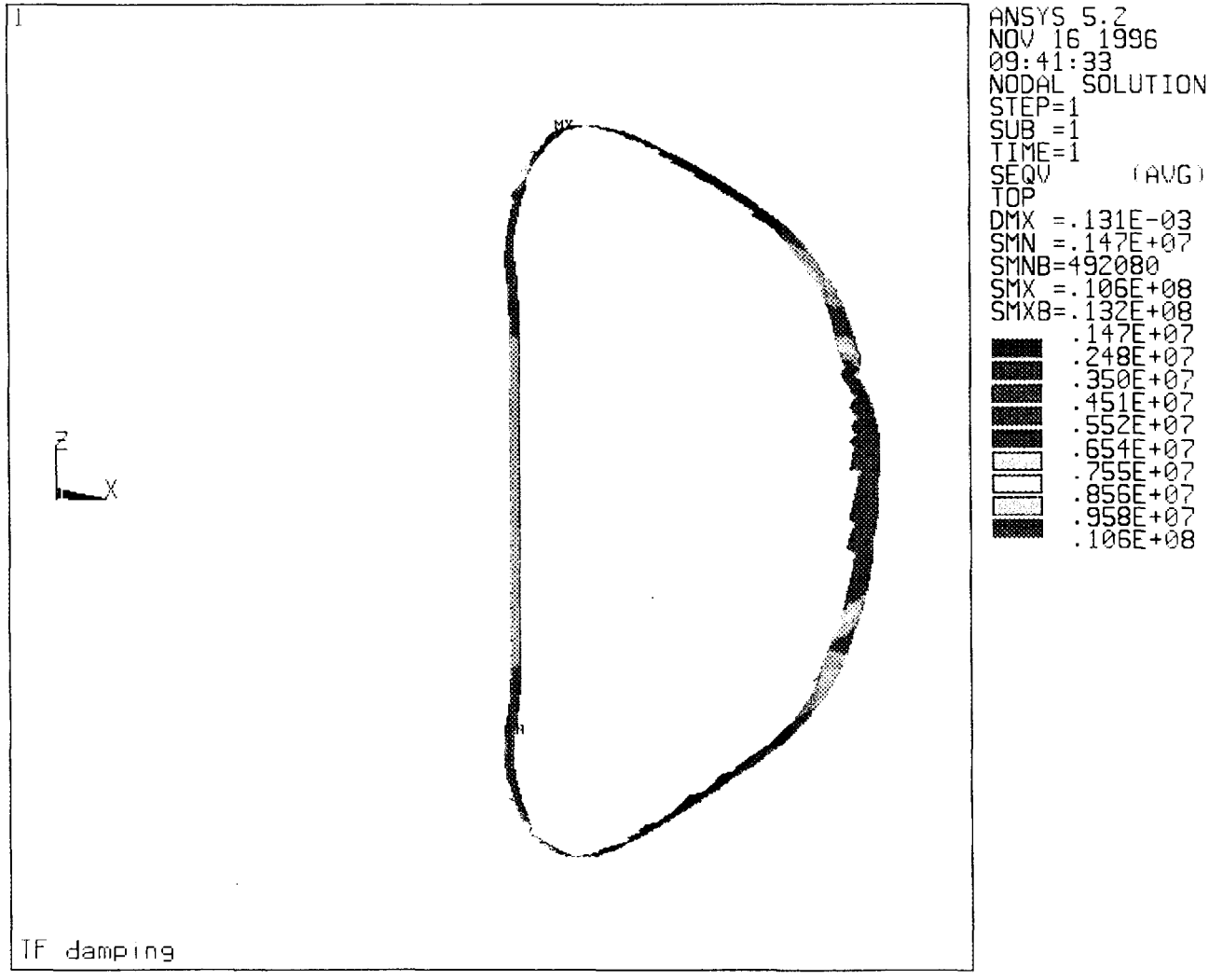

Fig. 19. Stress distribution on a poloidal belt section in TF damping.

Fig. 20. Stress distribution due to diamagnetism change during energy quench.

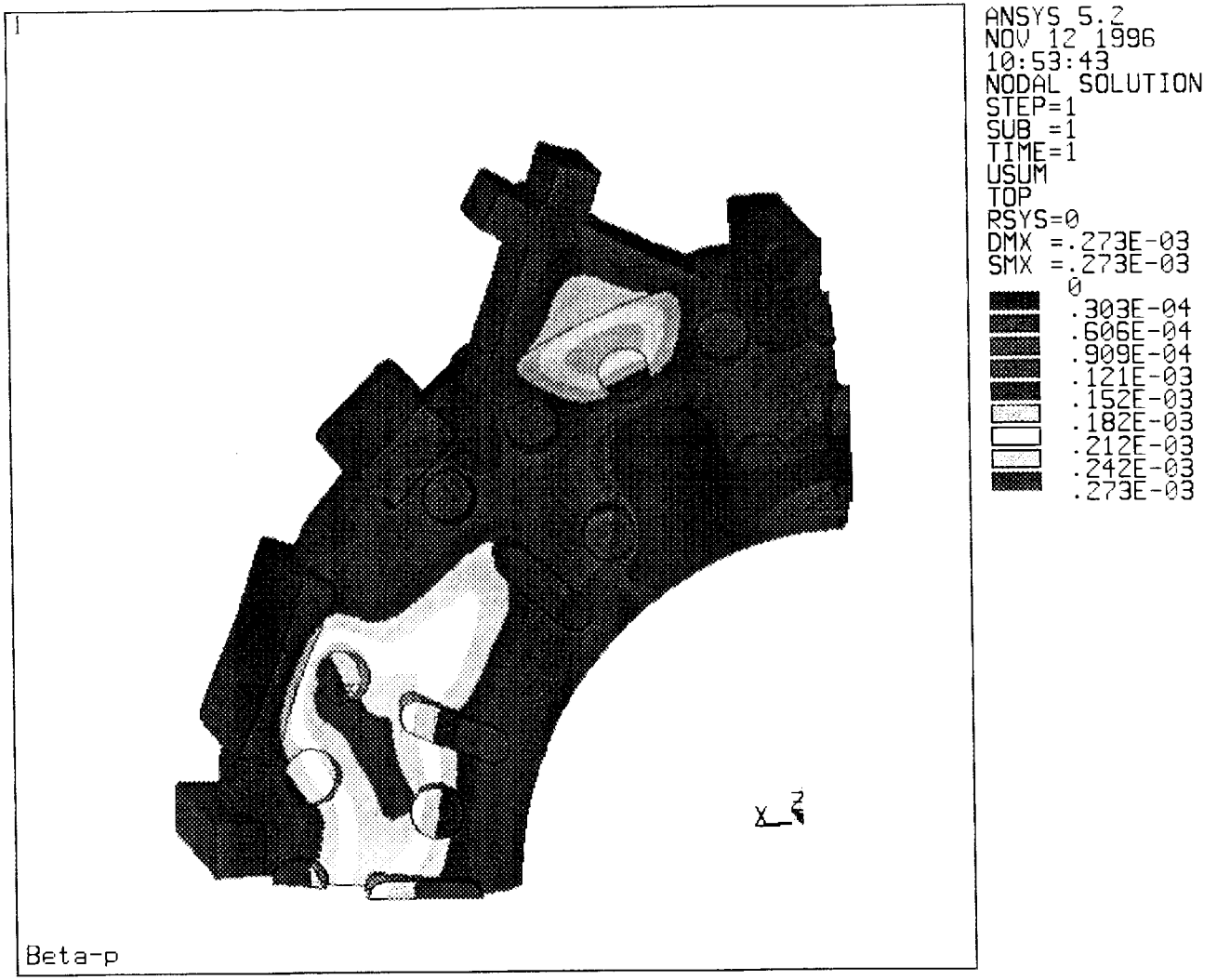

Fig. 21. Deformation of the vessel during energy quench.

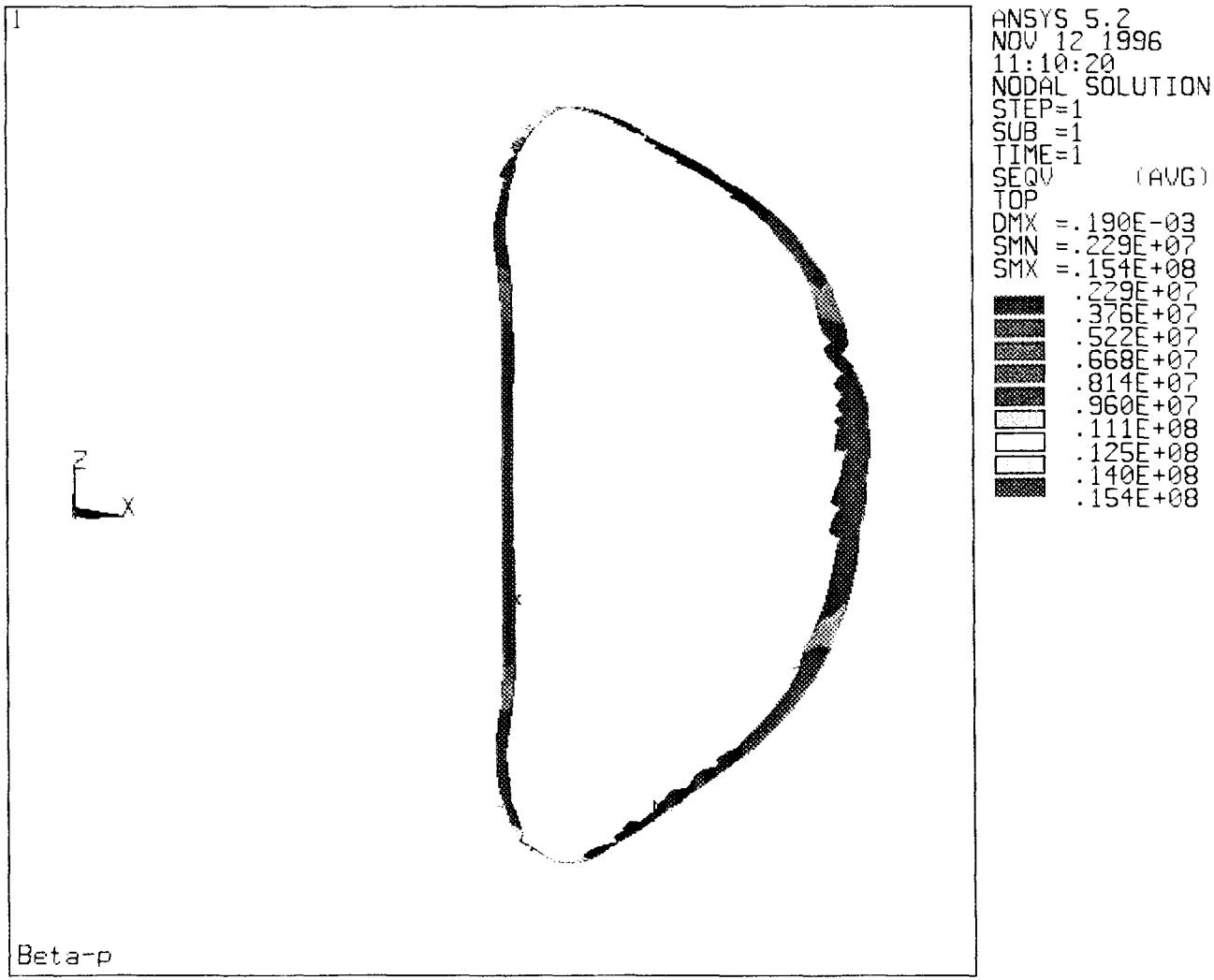

Fig. 22. Stress distribution on a poloidal belt section in the energy quench.

The maximum stress is 0.680×10^8 Pa. This value is not so larger than expected considering that in the mode of TF damping, because the stress concentration is occurred around the NBI port(large major radius side) where the magnitude and resultant effect of induced pressures of $1/r^2$ form are much lower than those of the atmospheric pressure. The maximum deformation is 0.273 mm.

Fig. 22 is the stress distribution on a poloidal belt section like as Fig. 19. As comparing the stresses on the linear part of the vessel($\theta \sim 180^\circ$) in the Figures 19 and 22, there is a large difference by ~2 (equivalent to the ratio of the pressures exerted) between two values, which represents that the stress analysis has been performed properly.

V. Conclusions

Analytic forms for the poloidal eddy currents flowing on the vessel, consequent pressures and forces acting on it were presented. The results were applied to typical operation modes of the KT-2 tokamak: machine start-up(TF coil charge), shut-down(discharge) and plasma disruption(diamgnetism change).

Stress anlysis for two typical operation modes of TF damping in the machine shut-down and plasma energy quench during the plasma disruption were carried out using 3D FEM code(ANSYS 5.2). The results of the stress analysis are summarized as follows;

mode	Atmospheric pressure	TF damping	Energy Quench
Max. deformation	0.241 mm	0.223 mm	0.273 mm
Max. stress	0.612×10^8 Pa	0.558×10^8 Pa	0.680×10^8 Pa
Most part of vessel	$0.680 \times 10^7 \sim 0.272 \times 10^8$ Pa	$0.620 \times 10^7 \sim 0.248 \times 10^8$ Pa	$0.756 \times 10^7 \sim 0.302 \times 10^8$ Pa
Linear part of vessel		0.775×10^7 Pa	0.154×10^8 Pa

References

[1] R.Albamese, et al.,"Effects of the eddy currents for some design and interpretation problems in a tokamak",Proc. of 17th SOFT 1992,Elsevier,679(1993)

[2] P.Noll, et al.,"Forces on the JET vacuum vessel during disruption and consequent operational limits",Fusion Tech.,15,259(1989)

[3] R計劃デザインチーム,"核融合反☒プラズマ實驗裝置技術報告(VII)",名古屋大學プラズマ研究所, ch.4 (1984)

[4] R.J.Thome,J.M.Tarrh,"MHD and fusion magnets",John Wiley & Sons(1982)

[5] 핵융합로연구/토카막장치기술개발,KAERI/RR-1536/94.과학기술처(1995)

[6] J.Wesson,"Tokamak",Clarendron Press,p68(1987)

[7] J.Gernhardt,F.Schneider,"Design and electric compensation of a diamagnetic loop and its application in the ASDEX tokamak",IPP III/84,Max-Planck Institute(1986)

[8] V.D.Shafranov,'Determination of the parameters β I and li in a for arbitrary shape of plasma pinch cross-section",Plasma Physics,13,757(1971)

[9] J.A.Wesson, et al.,"Disruptions in JET",Nuclear Fusion,29,641(1989)

서 지 정 보 양 식			
수행기관보고서번호	위탁기관보고서번호	표준보고서번호	INIS주제코드
KAERI/TR-779/96			

제목 / 부제	Mechanical Impacts of Poloidal Eddy Currents on the Continuous Vacuum Vessel of a Tokamak
연구책임자 및 부서명	인 상 렬 (핵융합로 연구분야)
연 구 자 및 부서명	인 상 렬, 윤 병 주 (핵융합로 연구분야)

발 행 지	대 전	발행기관	한국원자력연구소	발행일	1996. 11
페 이 지	50 p.	도 표	유(0), 무( )	크 기	210mm X 297mm
참고사항					

비밀여부	공개(0), 비공개( ), _급비밀	보고서종류	기술보고서
연구위탁기관		계약 번호	

초록 (300단어 내외)

토카막 진공용기는 항상 대기압의 영향을 받는 것이외에 플라즈마 발생과 소멸까지운전모드별로 각종의 전자기력을 받는다. TF 전자석 충전, TF 전자석 방전과 플라즈마 붕괴시의 energy quench의 모드에서 진공용기의 폴로이달 유기 전류가 발생한다. 용기에 흐르는 유기전류에 대한 일반적인 식과 그 전류로 인한 힘과 압력이 본 보고서에 표현되어 있습니다. 그 결과는 KT-2 토카막 운전시나리오에 적용된다.

TF 전자석 방전과 플라즈마 붕괴시의 energy quench의 모드에서 생성되는 두 가지 전자기력에 관하여 3D FEM 코드인 ANSYS 5.2를 사용하여 진공용기의 응력해석을 수행하였습니다.

주제명 키워드 (10단어 내외)

eddy current, vacuum vessel, TF, KT-2, plasma, disruption, tokamak, scenario

BIBLIOGRAPHIC INFORMATION SHEET					
Performing Org. Report No.	Sponsoring Org. Report No.		Standard Report NO.		INIS Subject Code
KAERI/TR-779/96					
Title / Subtitle	Mechanical Impacts of Poloidal Eddy Currents on the Continuous Vacuum Vessel of a Tokamak				
Project Manager and Dept.	Sang Ryul In (Nuclear Fusion Lab.)				
Researcher and Dept.	Sang Ryul In (Nuclear Fusion Lab.) Byung Joo Yoon (Nuclear Fusion Lab.)				
Pub.Place	Taejon	Pub. Org.	KAERI	Pub.Date	1996. 11
Page	50 p.	Fig. and Tab.	Yes(0), No( )	Size	210mm X 297mm
Note					
Classified	Open(0), Outside( ), _Class		Report Type		Technical Report
Sponsoring Org.			Contract No.		

Abstract (About 300 words)

Poloidal eddy currents are induced on the continuous torus vacuum vessel by changes of the toroidal field during the machine start-up(toroidal field coil charge), shut-down(toroidal field coil discharge) and plasma disruption(plasma diamgnetism change). Analytic forms for the eddy currents flowing on the vessel, consequent pressures and forces acting on it are presented in this report. The results are applied to typical operation modes of the KT-2 tokamak.

Stress analysis for two typical operation modes of toroidal field damping during a machine shut-down and plasma energy quench during a plasma disruption were carried out using 3D FEM code(ANSYS 5.2).

Subject Keywords (About 10 Words)

eddy current, vacuum vessel, TF, KT-2, plasma, disruption, tokamak, scenario